# Security-Reliability Trade-Offs for Satellite-Terrestrial Relay Networks with a Friendly Jammer and Imperfect CSI

Tan N. Nguyen, *Member, IEEE*, Trinh Van Chien, *Member, IEEE*, Dinh-Hieu Tran, Van-Duc Phan, Miroslav Voznak, *Senior Member, IEEE*, Symeon Chatzinotas, *Senior Member, IEEE*, Zhiguo Ding, *Fellow, IEEE*, and H. Vincent Poor, *Life Fellow, IEEE*

***Abstract*—This paper proposes and analyzes the reliability and security trade-off for a satellite-terrestrial (SatTer) relay system. Herein, a satellite sends confidential information to multiple ground users (GUs) with the help of a relay base station (BS) in the presence of multiple eavesdroppers trying to wiretap the information. In particular, a friendly jammer is deployed near the relay BS to improve secure transmissions. Moreover, the non-identical Rayleigh fading channels and imperfect channel state information (CSI) are adopted for a general system model. Then, we consider both amplify-and-forward (AF) and decode-and-forward (DF) relaying strategies to give a full picture of the benefits of each method. In this context, we derive the closed-form expressions of the outage probability (OP) and intercept probability (IP) corresponding to AF- and DF-based relaying schemes, which is a high challenge and has not been investigated before. Then, Monte-Carlo simulations are conducted to evaluate the correctness of the mathematical analysis and the effectiveness of the proposed methods. Furthermore, the security and reliability trade-off of the SatTer system and the influences of various system parameters (e.g., satellite's transmit power, channel estimation errors, relay's transmit power, fading severity parameter, the average power of light-of-sight, and satellite's multi-path components) on the system performance are shown.**

***Index Terms*—Amplify-and-forward, decode-and-forward, friendly jammer, non-identical Rayleigh, imperfect CSI, physical layer security, relay networks.**

## I. Introduction

The internet of things (IoT) is becoming an indispensable component in modern life, enabling a variety of amenities such as wearable devices, smart cities, self-driven cars, smart grids, smart farming, and healthcare [1], [2]. As reported by Ericsson, the number of IoT devices (IoTD) is predicted to reach around 26.9 billion by 2026 [3]. Nevertheless, the swift growth of the number of IoTD has presented many new challenges for current communication systems due to the limitations on resources, e.g., frequencies, power, poor flexibility. For instance, in the case of natural catastrophes or when the terrestrial base stations (BSs) are overloaded during peak hours, or they provide poorly data transmission in harsh environments, e.g., deserts, mountains, or maritime [4]–[6]. Fortunately, satellite communications (SatCom) have recently emerged as a promising solution to overcome the above issues. It is because SatCom can provide universal coverage and, together with terrestrial communications (TerCom) to support a massive number of IoTD. Recently, many projects, such as OneWeb, SPUTNIX, Kepler, and SpaceX, have planed to bring hundreds of LEO satellites in the sky to provide high throughput and global communications [7].

Beyond many advantages, a large distance between satellites and ground users (GUs) imposes new challenges. One of them is the masking effect in Satcom, in which a GU is unable to receive the satellite signals because the line-of-sight (LoS) is obscured, e.g., due to fog attenuation and the GU in a building or a tunnel. Therefore, satellite-terrestrial relay networks (STRN) have received considerable attention from researchers to leverage space resources for communications. Specifically, relay node in cooperative networks helps transfer information between GUs. It thus benefits the coverage for IoTD with limited power and locates far away. The cooperative networks can be classified into two main types, termed amplify-and-forward (AF)-based relaying [8] and decode-and-forward (DF)-based relaying [9], [10]. In the literature, there also exist other methods such as hybrid AF and DF (HAD) [11], or randomize-and-forward [12].

The concept of STRN was first introduced by Chamberlain and Medhurst in 1965 [13], [14], and 1966 [15]. Lee et al. [16] were the first to introduce the symbiosis between TerCom and SatCom in 1983. Carlo et al. [17] investigated the co-channel interference (CCI) in a satellite-terrestrial integration system. Recently, STRN still attracts researchers from academia to industry since it is a promising direction for future sixth-generation (6G) networks [18]. Two-way satellite relaying has been investigated in [19]–[21]. In [19], the authors used a satellite as a relay to transfer information between two ground BSs, whereas each BS applied different modulation schemes to avoid the difficulty of channel estimation. Zeng et al. [20] studied the performance analysis of a two-way satellite-terrestrial (SatTer) system, where the satellite-relay link followed $\kappa - \mu$ shadowed fading, and relay-GU link is Nakagami-m fading channels. Kefeng et al. [21] analyzed

Manuscript received xxx; revised xxx and xxx; accepted xxx. Date of publication xxx; date of current version xxx. This study was financially supported by Van Lang University, Vietnam. This research is funded by Hanoi University of Science and Technology (HUST) under project number T2022-TT-001 for Trinh Van Chien. The work of H. V. Poor was supported by U.S National Science Foundation under Grant CNS-2128448. This work was supported in part by the Ministry of Education, Youth and Sports of the Czech Republic under Grant SP2022/5, and in part by e-INFRA CZ under Grant 90140. The associate editor coordinating the review of this article and approving it for publication was K. Amit. (Corresponding author: Van-Duc Phan.)

T. N. Nguyen is with Communication and Signal Processing Research Group, Faculty of Electrical and Electronics Engineering, Ton Duc Thang University, Ho Chi Minh City, Vietnam. (e-mail:nguyennhattan@tdtu.edu.vn).

T. V. Chien is with the School of Information and Communication Technology (SoICT), Hanoi University of Science and Technology (HUST), 100000 Hanoi, Vietnam (e-mail: chientv@soict.hust.edu.vn).

D. H. Tran is with Nokia Bell Labs, France (email:dinh-hieu.tran@nokia.com).

Van-Duc Phan is with the Faculty of Automotive Engineering, School of Engineering and Technology, Van Lang University, Ho Chi Minh City, Vietnam (email: duc.pv@vlu.edu.vn).

M. Voznak is with VSB - Technical University of Ostrava, 17. listopadu 15/2172, 708 33 Ostrava - Poruba, Czech Republic. (e-mail:miroslav.voznak@vsb.cz).

Z. Ding is with the School of Electrical and Electronic Engineering, The University of Manchester, Manchester M13 9PL, U.K. (e-mail: zhiguo.ding@manchester.ac.uk).

H. V. Poor is with the Electrical Engineering Department at Princeton University, NJ 08544, (email: poor@princeton.edu).

the performance of a two-way SatTer communication under the influence of the hardware impairments. Dong et al. [22] studied the intelligent reflecting surface (IRS)-assisted SatTer system in which an IRS acted as a relay to reflect signals from ground BSs and satellite. In [23], [24], the authors investigated the space-air-terrestrial communications. Specifically, Tran et al. [24] proposed a novel system model with two tiers communication system, whereas the cache-enabled unmanned aerial vehicle (UAV) was deployed as a relay to transfer information from a satellite to GUs. If the requested files were stored at the UAV, then it transmitted directly to GUs. Otherwise, the UAV demanded the requested files from the satellite on the backhaul link. Sharma et al. [23] employed an AF-based three-dimensional (3D) UAV relay between satellite and GU.

The issue of security in SatTer networks has raised as an important factor that need to be solve, especially for confidential information or in military applications. Due to a high simplicity and ease to implement in practice, physical layer security (PLS) for wireless communications has gained great attraction from research community [25]–[28]. Besides, PLS was also applied in SatTer networks recently [29]–[32]. Bankey et al. [29] investigated a downlink SatTer network including multiple satellites, multiple relays, multiple destinations, and multiple eavesdroppers. Kalantari et al. [30] studied the security issue in a bidirectional satellite system applying network coding to exchange information between two GUs. Sharma et al. [31] investigated a secure transmission in SatTer networks, where UAVs were deployed as relays to transfer information between a satellite and a GU. The security problem for IRS-enabled SatTer communications was proposed and analyzed in [32]. Specifically, an IRS was installed near the GU to protect the satellite's confidential information from the eavesdropper. Despite many advantages, none of the above works [29]–[32] consider jammer or artificial noise to improve the secure transmission in SatTer networks. Recently, there are only some works that bring jammers to SatTer wireless communication systems [33]–[35]. In 1996, Kai-Bor was the first one who introduced jammer in satellite communications. Specifically, he developed an algorithm to control beamforming and jamming protection. Mounia et al. [34] investigated the PLS of SatTer Cognitive networks in the presence of a friendly jammer. Bankey et al. [35] applied a UAV-based friendly jammer to improve the security of satellite communications.

Motivated from the above discussions, we aim at this work to analyze the security-reliability trade-off in a SatTer communication consisting of one satellite S that is communicating with multiple GUs through the help of a relay. Moreover, there exists multiple eavesdroppers that try to overhear the confidential information from the relay. Besides, a friendly jammer is deployed in the system to enhance the system security by transmit jamming signals to eavesdroppers. Particularly, the channels from satellite to relay and from relay to GUs follow shadowed Rician and non-identical Rayleigh fading, respectively. The contributions of our work can be pointed out as follows:

- To the best of our knowledge, this is the first work that investigates the security-reliability trade-off in SatTer relay networks with a friendly jammer and imperfect channel state information (CSI), whereas the channels of satellite and terrestrial links are Shadow-Rician fading and non-identical Rayleigh channels, respectively.
- The intensive analyses for security and reliability trade-off are performed under influences of different network parameters. Moreover, we first derive the closed-formed expressions for outage probability (OP) and intercept probability (IP). Particularly, both AF and DF relaying networks are taken into account to fully investigate the performance of each method.
- Numerical and simulation results are provided to insightful discussions on the effects of various critical parameters such as satellite's transmit power, channel estimation errors, relay's transmit power, fading severity parameter, the average power of LoS, and multi-path components of the satellite. The results give helpful guidance to design a system in practice to satisfy the reliability with an acceptable intercept performance.

The security and reliability trade-off for the satellite-terrestrial relay networks has recently attracted interest, for example, our recent publication [36] and references therein. Regarding the system model, in [36], the best relay is selected to receive the transmitted signals from the satellite under the influences of an eavesdropper. The presence of a jammer contributes to both legitimate and illegitimate devices (please refer to [36, Fig. 1]). The closed-form expressions of the OP and IP were obtained under imperfect CSI, but the previous work only investigated system performance with AF.

In the current work, we have shared the same satellite-terrestrial literature with the previous works [36], [37], especially the reliability and security issues [36]. However, this paper is more general than [36] since the fading channels are applied for arbitrary locations of the eavesdroppers and the destinations. Specifically, three fundamental differences exist between the current work and [36]. First, we investigate multiple eavesdroppers and multiple destinations, while [36] considered the single eavesdropper and destination. Second, we consider the influences of both the AF and DF technologies, while [36] considered the former only. Finally, the non-identical fading channels are utilized in the current paper, while the independent and identically distributed shadow fading model for the communication between the satellite and relay was considered in [36].

## II. System Model

In Fig. 1, we present the system model considering in our paper consisting of one satellite S, a BS that acts as a relay R, and multiple destinations $\mathrm{D}_n$ with $n \in \{1, \ldots, N\}$ in the presence of one jammer and multiple eavesdroppers. All destinations are assumed in the coverage area of the satellite S, but they cannot leverage the direct link to satellite because they are not equipped with expensive high-gain antennas [24], [38]. In this system model, the satellite S transmits its signals to the destinations $\mathrm{D}_n$ with the help of one relay R. Moreover, relay R performs the AF and DF techniques to relay the information to destinations $\mathrm{D}_n$. In the meantime, adversary E tries to wiretap the confidential information from relay R.

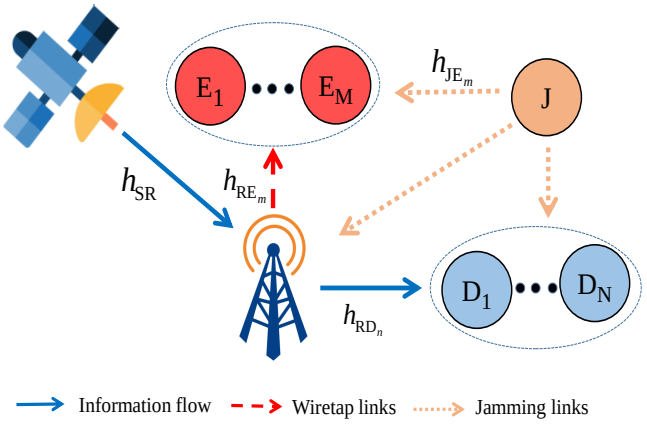


Fig. 1. The considered system model.

To improve the network security, a friendly jammer is installed to create artificial noises, reducing the eavesdropper's impact.

### A. Channel Model

Herein, the characterizations for fading channels is given as follows. It is assumed that the estimated channels between two arbitrary nodes in terrestrial links follow the block Rayleigh fading model, where channel coefficients are constant during one transmission block and change independently over different transmission blocks. The block Rayleigh fading channels match well with practical environments where the transceivers are surrounded by many scatterers, which were confirmed by practical measurements in [39], [40].[1] Because the channels are Rayleigh fading, their channel gains can be expressed as $\gamma_{\mathrm{RE}_m} = |h_{\mathrm{RE}_m}|^2, \gamma_{\mathrm{RD}_n} = |h_{\mathrm{RD}_n}|^2$, etc., are exponential random variables (RVs), where cumulative distribution function (CDF) and probability density function (PDF) are respectively given as follows

$$F_X(x) = 1 - \exp(-\lambda x), \tag{1}$$

$$f_X(x) = \frac{\partial F_X(x)}{\partial x} = \lambda \exp(-\lambda x), \tag{2}$$

where $\lambda$ is the rate parameter of the exponential RV $X$.

For satellite links, we consider shadowed-Rician fading model [41].[2] Then, the PDF of channel gain $\gamma_{\mathrm{SR}} = |h_{\mathrm{SR}}|^2$ between satellite and relay is given by [29], [43]

$$f_{\gamma_{\mathrm{SR}}}(x) = \alpha \exp(-\beta x)\, {}_1F_1(m_s; 1; \delta x), x \geq 0, \tag{3}$$

where $\alpha = \beta\left(\frac{2bm_s}{2bm_s+\Omega_s}\right)^{m_s}, \beta = \frac{1}{2b}$, and $\delta = \frac{\beta\Omega_s}{2bm_s+\Omega_s}$, with $\Omega_s$ and $2b$ are the average power of LoS and multi-path components, respectively. Herein, $m_s$ is the fading severity parameter and ${}_1F_1(\cdot;\cdot;\cdot)$ is the confluent hypergeometric function of the first kind [44, Eq. 9.210.1]. For arbitrary integer-valued fading severity parameters, one can simplify ${}_1F_1(m_s; 1; \delta x)$ in (3) to express the PDF of $\gamma_{\mathrm{SR}}$ [45] as follows

$$f_{\gamma_{\mathrm{SR}}}(x) = \alpha \sum_{k=0}^{m_s-1} \zeta(k) x^k \exp(-(\beta-\delta)x), \tag{4}$$

where $\zeta(k) = \frac{(-1)^k (1-m_s)_k \delta^k}{(k!)^2}$ with $(\cdot)_k$ is the Pochhammer symbol [44, page xliii]. Based on (4), the corresponding CDF $F_{\gamma_{\mathrm{SR}}}(x) = \Pr(\gamma_{\mathrm{SR}} < x) = \int_0^x f_{\gamma_{\mathrm{SR}}}(x)dx$ can be obtained by applying [44, Eq. 3.351.1] as follows:

$$F_{\gamma_{\mathrm{SR}}}(x) = 1 - \alpha \sum_{k=0}^{m_s-1} \sum_{p=0}^{k} \frac{\zeta(k)k!}{p!} (\beta-\delta)^{-(k+1-p)} \times x^p \exp(-(\beta-\delta)x). \tag{5}$$

The configuration of the satellite link, the analysis in this paper can be applied for various configurations because our model focuses on the outage and secrecy performance, which depends mainly on the channel statistical properties. This paper will select a practical case for our numerical analysis by the satellite link to support 5G-and-beyond applications as the review of satellite frequency bands in Europe [46]. More specifically, this paper concentrates on the Ka-band (17.7-20.2 GHz space-to-Earth and 27.5-30 GHz Earth-to-space). Specifically, the carrier frequency is chosen as 28 GHz for the analysis. It is recommended to use highly directional antennas for antenna configuration to reduce interference. For example, horn, slotted waveguide array, and microstrip patch array antennas are deployed for cellular links, and dish antennas are for satellite links [47], [48]. In practice, it is difficult to obtain perfect CSI due to some channel estimation errors (CEEs). Thus, some channel estimation algorithms are necessary to obtain CSI, e.g., linear minimum mean square error (MMSE) method [49]. Therefore, channels can be modeled as [50]

$$\widehat{h}_i = h_i + e_i, \tag{6}$$

where $e_i$, $i \in (\mathrm{SR}, \mathrm{RD}_n, \mathrm{RE}_m, \mathrm{JE}_m, \mathrm{JR}, \mathrm{JD}_n)$ is the CEE with $e_i \sim CN(0, \mu_i^2)$, $h_i$ is the estimated channel of real channel $\widehat{h}_i$.

### B. AF Relaying Protocol

This section discusses the AF relaying protocol, where the relay R first amplifies the received signal and then transfers it to the destination D. Because all system nodes are performed in a half-duplex (HD) mode, the signal transmission from satellite to destination during two time slots. In the first time slot, satellite transmits its signal $x_{\mathrm{S}}$ to the relay BS. Therefore, the received signal at R can be given by

$$y_{\mathrm{R}} = \widehat{h}_{\mathrm{SR}} x_{\mathrm{S}} + n_{\mathrm{R}} = (h_{\mathrm{SR}} + e_{\mathrm{SR}}) x_{\mathrm{S}} + n_{\mathrm{R}}, \tag{7}$$

where $x_{\mathrm{S}}$ is the transmit signal of satellite with $\mathrm{E}\{\|x_{\mathrm{S}}\|\}^2 = P_{\mathrm{S}}$, $\mathrm{E}\{\cdot\}$ is the expectation operation; $n_{\mathrm{R}}$ is the zero mean additive white Gaussian noise (AWGN) with variance $\mathrm{N}_0$.

In the second time slot, relay BS amplifies received signal $y_{\mathrm{R}}$ and then conveys it to the chosen destination $\mathrm{D}_n$. During this time, the eavesdroppers track the signal transmitted from BS R and try to wiretap the information. To reduce the quality of the eavesdropping link, the cooperative jamming technique can be used, where the single antenna friendly

[1] This paper provides an initial analytical framework for balancing security and reliability in the satellite-terrestrial relay networks. The terrestrial links follow the Rayleigh fading model suitable without a dominant path. An extension to a general fading channel model such as the Nakagami-m fading channel should be of interest for future work.

[2] The shadowed Rician model considers a Rician fading channel through LoS shadowing and the rich scattering environment around relay. Physically, this fading model is applied for the propagation scenarios where objects moving near relay make the received signal power be shadowed, which is a greater extent than the signal power given through the direct channel between the satellite and relay [42].

jammer (J) is employed to continuously generate the artificial noises to eavesdroppers. Because of the masking effect, it is almost impossible for the eavesdroppers to overhear the signal from the satellite directly. Therefore, it is assumed that eavesdroppers monitor only transmitted signals from terrestrial relay BS [29], [51]. Consequently, the obtained signal at the $n$-th destination and the $m$-th eavesdropper can be given as

$$y_{\mathrm{D}_n}^{\mathrm{AF}} = \left(h_{\mathrm{RD}_n} + e_{\mathrm{RD}_n}\right) \mathrm{G} \left(\left(h_{\mathrm{SR}} + e_{\mathrm{SR}}\right) x_{\mathrm{S}} + n_{\mathrm{R}}\right) + n_{\mathrm{D}_n}, \tag{8}$$

$$y_{\mathrm{E}_m}^{\mathrm{AF}} = \left(h_{\mathrm{RE}_m} + e_{\mathrm{RE}_m}\right) \mathrm{G} \left(\left(h_{\mathrm{SR}} + e_{\mathrm{SR}}\right) x_{\mathrm{S}} + n_{\mathrm{R}}\right) + \left(h_{\mathrm{JE}_m} + e_{\mathrm{JE}_m}\right) x_{\mathrm{J}} + n_{\mathrm{E}_m}, \tag{9}$$

where $n_{\mathrm{D}_n}$ and $n_{\mathrm{E}_m}$ are the zero mean AWGN with variance $\mathrm{N}_0$ at the n-th user and m-th eavesdropper, respectively; $x_{\mathrm{J}}$ is the transmitted signal at J and is satisfied $\mathrm{E}\left\{\left|x_{\mathrm{J}}\right|^2\right\} = P_{\mathrm{J}}$. Based on (7), the amplify factors G at relay R are determined as

$$\mathrm{G} = \sqrt{\frac{P_{\mathrm{R}}}{P_{\mathrm{S}}\left(\gamma_{\mathrm{SR}} + \mu_{\mathrm{SR}}^2\right) + N_0}}. \tag{10}$$

From (8), (9) and (10), the signal to noise ratio (SNR) at the $n$-th user and the $m$-th eavesdropper can be respectively expressed as

$$\gamma_{\mathrm{D}_n}^{\mathrm{AF}} = \frac{\Psi\Phi\gamma_{\mathrm{SR}}\gamma_{\mathrm{RD}_n}}{\gamma_{\mathrm{RD}_n}\Phi\left(\mu_{\mathrm{SR}}^2\Psi + 1\right) + \gamma_{\mathrm{SR}}\Psi\vartheta_3 + \Xi}, \tag{11}$$

$$\gamma_{\mathrm{E}_m}^{\mathrm{AF}} = \frac{\Psi\Phi\gamma_{\mathrm{SR}}\gamma_{\mathrm{RE}_m}}{\gamma_{\mathrm{RE}_m}\Phi\vartheta_1 + \gamma_{\mathrm{SR}}\Psi\vartheta_2 + \gamma_{\mathrm{JE}_m}\Theta\vartheta_1 + \Lambda}, \tag{12}$$

where $\Psi \triangleq \frac{P_{\mathrm{S}}}{N_0}$; $\Phi \triangleq \frac{P_{\mathrm{R}}}{N_0}$; $\Theta \triangleq \frac{P_{\mathrm{J}}}{N_0}$; $\Xi \triangleq \left(\Psi\mu_{\mathrm{SR}}^2 + 1\right)\left(\Phi\mu_{\mathrm{RD}_n}^2 + 1\right)$, $\vartheta_1 \triangleq \left(\mu_{\mathrm{SR}}^2\Psi + 1\right)$, $\vartheta_2 \triangleq \left(\mu_{\mathrm{RE}_m}^2\Phi + \Theta\mu_{\mathrm{JE}_m}^2 + \Theta\gamma_{\mathrm{JE}_m} + 1\right)$, $\vartheta_3 \triangleq \left(\mu_{\mathrm{RD}_n}^2\Phi + 1\right)$, and $\Lambda \triangleq \left(\Psi\mu_{\mathrm{SR}}^2 + 1\right)\left(\Phi\mu_{\mathrm{RE}_m}^2 + \Theta\mu_{\mathrm{JE}_m}^2 + 1\right)$.

### *C.* DF Relaying Protocol

This subsection describes the DF relaying protocol, whereas the terrestrial BS first decodes the received signal from the satellite and then re-encodes and transmits the decoded signal to the destination. In the first phase, the satellite S broadcasts its signal $x_{\mathrm{S}}$ to relay, and the received signal at the relay is the same as (7). Based on (7), the SNR at R can be expressed as $\gamma_{\mathrm{R}} = \frac{\Psi\gamma_{\mathrm{SR}}}{\vartheta_1}$. Then, the total data transmission rate from $\mathrm{S} \to \mathrm{R}$ is calculated as:

$$C_{\mathrm{R}} = \frac{1}{2}\log_2\left(1 + \gamma_{\mathrm{R}}\right). \tag{13}$$

As the definition of DF relaying [29], for a specific terrestrial BS R, if $C_{\mathrm{R}}$ is larger than a predefined rate threshold $C_{\mathrm{th}}$, BS R can successfully decode the satellite signal and it then forward this information to the destination in the second time slot. In the second time slot, BS R forwards the decoded signal to a chosen destination that has the best channel. Therefore, the signal received from $n$-th user and $m$-th eavesdropper are respectively expressed as

$$y_{\mathrm{D}_n}^{\mathrm{DF}} = \left(h_{\mathrm{RD}_n} + e_{\mathrm{RD}_n}\right) x_{\mathrm{R}} + n_{\mathrm{D}_n}, \tag{14}$$

$$y_{\mathrm{E}_m}^{\mathrm{DF}} = \left(h_{\mathrm{RE}_m} + e_{\mathrm{RE}_m}\right) x_{\mathrm{R}} + \left(h_{\mathrm{JE}_m} + e_{\mathrm{JE}_m}\right) x_{\mathrm{J}} + n_{\mathrm{E}_m}. \tag{15}$$

From (14) and (15), the SNRs at $n$-th user and $m$-th eavesdropper are respectively given as:

$$\gamma_{\mathrm{D}_n}^{\mathrm{DF}} = \min\left(\gamma_{\mathrm{R}}, \gamma_{\mathrm{RD}_n}\right) = \min\left(\frac{\Psi\gamma_{\mathrm{SR}}}{\vartheta_1}, \frac{\Phi\gamma_{\mathrm{RD}_n}}{\Phi\mu_{\mathrm{RD}_n}^2 + 1}\right), \tag{16}$$

$$\gamma_{\mathrm{E}_m}^{\mathrm{DF}} = \min\left(\frac{\Psi\gamma_{\mathrm{SR}}}{\vartheta_1}, \frac{\Phi\gamma_{\mathrm{RE}_m}}{\vartheta_4}\right), \tag{17}$$

where $\vartheta_4 \triangleq \Theta\gamma_{\mathrm{JE}_m} + \Theta\mu_{\mathrm{JE}_m}^2 + \Phi\mu_{\mathrm{RE}_m}^2 + 1$, $\gamma_{\mathrm{RD}_n} = \frac{\Phi\gamma_{\mathrm{RD}_n}}{\Phi\mu_{\mathrm{RD}_n}^2 + 1}$ is the SNR at $\mathrm{D}_n$ to decode successfully $x_{\mathrm{R}}$.

**Remark 1:** The best destination $\mathrm{D}_n$ would be selected for the purpose of improving transmission performance. Mathematically speaking, the best $n$-th destination can be selected as follows

$$n = \arg \underbrace{\max}_{q=1,2,\ldots,N} \left\{\gamma_{\mathrm{RD}_q}\right\} \Leftrightarrow \gamma_{\mathrm{RD}_n} = \underbrace{\max}_{q=1,2,\ldots,N} \left\{\gamma_{\mathrm{RD}_q}\right\}, \tag{18}$$

Assume that the transmission links from R to $N$ destinations nodes are independent non-identical distribution (i.n.i.d) Rayleigh fading channels such that $\lambda_{\mathrm{RD}_n} \neq \lambda_{\mathrm{RD}_q}, \forall n \neq q$. Therefore, the CDF of $\gamma_{\mathrm{RD}_n}$ can be formulated as follows [52]:

$$F_{\gamma_{\mathrm{RD}_n}}(x) = \Pr\left(\gamma_{\mathrm{RD}_n} < x\right) = \prod_{q=1}^{N} F_{\gamma_{\mathrm{RD}_q}}(x)$$
$$= 1 + \sum_{q=1}^{N}(-1)^q \sum_{1 \le j_1 \le \cdots \le j_q \le N} \exp\left(-\sum_{i=1}^{q} \lambda_{\mathrm{RD}_{j_i}} x\right). \tag{19}$$

**Remark 2:** In this model, we adopt a non-colluding (N-COL) eavesdroppers scenario. It means that eavesdroppers are not able to exchange signals with each other; thus, they cannot cooperate to strengthen the received signals. This means that the system security can be achieved when the quality of the legitimate channel is superior to that of any eavesdropper's channel [53]. Therefore, the signal-to-noise ratios (SNRs) at eavesdroppers, for $l \in \{\mathrm{AF}, \mathrm{DF}\}$, are expressed as [29], [54]:

$$\gamma_{\mathrm{E}_m}^{l,\mathrm{N-COL}} = \max_{m=1,\ldots,M} \left\{\gamma_{\mathrm{E}_m}^{l}\right\}. \tag{20}$$

Furthers, it can be realized from (12) that $\gamma_{\mathrm{E}_m}^{\mathrm{AF}}$ is an increasing function with respect to $\gamma_{\mathrm{RE}_m}$. Thereby, for $l$ = AF, (14) can be considered as [55]:

$$\gamma_{\mathrm{E}_m}^{\mathrm{AF,N-COL}} = \frac{\Psi\Phi\gamma_{\mathrm{SR}}\gamma_{\mathrm{RE}_m}^{\mathrm{N-COL}}}{\gamma_{\mathrm{RE}_m}^{\mathrm{N-COL}}\Phi\vartheta_1 + \gamma_{\mathrm{SR}}\Psi\vartheta_2 + \gamma_{\mathrm{JE}_m}\Theta\left(\Psi\mu_{\mathrm{SR}}^2 + 1\right) + \Lambda}, \tag{21}$$

where $\gamma_{\mathrm{RE}_m}^{\mathrm{N-COL}} = \max_{m=1,\ldots,M} \left\{\gamma_{\mathrm{RE}_m}\right\}$.

Sequentially, according to the DF relaying protocol, (17) can be expressed as follows:

$$\gamma_{\mathrm{E}_m}^{\mathrm{DF,N-COL}} = \min\left(\frac{\Psi\gamma_{\mathrm{SR}}}{\vartheta_1}, \frac{\Phi\gamma_{\mathrm{RE}_m}^{\mathrm{N-COL}}}{\vartheta_4}\right). \tag{22}$$

Since we consider i.n.i.d channel from R to the M eavesdroppers nodes. Similar to (19), the CDF of $\gamma_{\mathrm{RE}_m}^{\mathrm{N-COL}} =$

$\max\limits_{m=1,\ldots,M}\{\gamma_{\mathrm{RE}_m}\}$ can be written by:

$$F_{\gamma_{\mathrm{RE}_m}^{\mathrm{N-COL}}}(x) = 1+\sum_{t=1}^{M}(-1)^t \sum_{1\le j_1\le\cdots\le j_q\le M} \exp\left(-\sum_{i=1}^{t}\lambda_{\mathrm{RE}_{j_i}}x\right). \quad (23)$$

## III. Performance Analysis

This section derives the OP and IP in closed-form expressions that only depend the channel statistics.

### A. AF Relaying Protocol

*1)* Outage Probability (OP) Analysis: The OP of system can be defined as

$$\mathrm{OP}^{l} = \Pr\left(\gamma_{\mathrm{D}_n}^{l} < \gamma_{th}\right) \quad (24)$$

where $l \in \{\mathrm{AF}, \mathrm{DF}\}$ and $\gamma_{\mathrm{th}} = 2^{2C_{th}}-1$ is the predefined rate threshold of the system. Based on (11) and (24), the $\mathrm{OP}^{\mathrm{AF}}$ can be calculated as

$$\begin{aligned}\mathrm{OP}^{\mathrm{AF}} &= \sum_{n=1}^{N}\Pr\left(\gamma_{\mathrm{RD}_n} = \max_{q=1,2,\ldots,N}\left(\gamma_{\mathrm{RD}_q}\right), \gamma_{\mathrm{D}_n}^{\mathrm{AF}} < \gamma_{th}\right)\\ &= \sum_{n=1}^{N}\underbrace{\Pr\left(\gamma_{\mathrm{RD}_n} > Z_n, \frac{\Psi\Phi\gamma_{\mathrm{SR}}\gamma_{\mathrm{RD}_n}}{\gamma_{\mathrm{RD}_n}\Phi\vartheta_1+\gamma_{\mathrm{SR}}\Psi\vartheta_3+\Xi} < \gamma_{th}\right)}_{\mathrm{Q}},\end{aligned} \quad (25)$$

where $Z_n \triangleq \max\limits_{q=1,2,\ldots,N,q\neq n}\left(\gamma_{\mathrm{RD}_q}\right)$.

*Lemma 1:* Based on (19), the CDF of $Z_n$ can be given as

$$\begin{aligned}F_{Z_n}(x) = \Pr\left(Z_n < x\right) &= \prod_{q=1,q\neq n}^{N}\left(1-\exp\left(-\lambda_{\mathrm{RD}_n}x\right)\right)\\ &= 1+\sum_{q=1}^{N-1}(-1)^q\widetilde{\sum}\exp\left(-\lambda_{n,q}^{\mathrm{sum}}x\right),\end{aligned} \quad (26)$$

where $\lambda_{n,q}^{\mathrm{sum}} = \sum\limits_{i=1}^{q}\lambda_{\mathrm{RD}_{j_i}}$, $\widetilde{\sum} \triangleq \sum\limits_{\substack{j_1=\cdots=j_q=1,\\ j_1<\cdots<j_q,\\ j_1,\ldots,j_q\neq n}}^{N}$.

Then the PDF of $Z_n$ can be obtained as

$$f_{Z_n}(x) = \sum_{q=1}^{N-1}(-1)^{q+1}\widetilde{\sum}\lambda_{n,q}^{\mathrm{sum}}\exp\left(-\lambda_{n,q}^{\mathrm{sum}}x\right). \quad (27)$$

*Lemma 2:* Q in (25) can be calculated as

$$Q = Q_1 + Q_2 + Q_3, \quad (28)$$

where

$$\begin{aligned}Q_1 &= \sum_{q=1}^{N-1}(-1)^{q+1}\widetilde{\sum}\int_0^{\infty}\lambda_{n,q}^{\mathrm{sum}}\exp\left(-z\widetilde{\lambda}^{\mathrm{sum}}\right)dz\\ &= \sum_{q=1}^{N-1}(-1)^{q+1}\widetilde{\sum}\frac{\lambda_{n,q}^{\mathrm{sum}}}{\widetilde{\lambda}^{\mathrm{sum}}},\end{aligned} \quad (29)$$

$$\begin{aligned}Q_2 = 1-\alpha\sum_{k=0}^{m_s-1}\sum_{p=0}^{k}\frac{\zeta(k)k!}{p!}(\beta-\delta)^{-(k+1-p)}\\ \times\left[\frac{\gamma_{th}\vartheta_1}{\Psi}\right]^p\exp\left(-\frac{\gamma_{th}\vartheta_1(\beta-\delta)}{\Psi}\right),\end{aligned} \quad (30)$$

$$Q_3 = Q_{31}+Q_{32}+Q_{33}, \quad (31)$$

with

$$\begin{aligned}Q_{31} = \sum_{q=1}^{N-1}(-1)^{q+1}\widetilde{\sum}\sum_{k=0}^{m_s-1}\sum_{p=0}^{k}\frac{\lambda_{n,q}^{\mathrm{sum}}}{\widetilde{\lambda}^{\mathrm{sum}}}\times\frac{\alpha\zeta(k)k!}{p!}\\ \times(\beta-\delta)^{-(k+1-p)}\left[\frac{\gamma_{th}\vartheta_1}{\Psi}\right]^p\exp\left(-\frac{(\beta-\delta)\gamma_{th}\vartheta_1}{\Psi}\right),\end{aligned} \quad (32)$$

$$\begin{aligned}Q_{32} = 2\sum_{q=1}^{N-1}(-1)^{q+1}\widetilde{\sum}\sum_{k=0}^{m_s-1}\sum_{p=0}^{k}\binom{k}{p}\frac{\alpha\zeta(k)[\gamma_{th}\vartheta_1]^{k-p}}{\Psi^{k+1}}\\ \times\exp\left(-\frac{(\beta-\delta)\gamma_{th}\vartheta_1}{\Psi}-\frac{\lambda_{\mathrm{RD}_n}\gamma_{th}\vartheta_3}{\Phi}\right),\\ \times\left\{\frac{\lambda_{\mathrm{RD}_n}\gamma_{th}\Psi\left[\gamma_{th}\vartheta_1\vartheta_3+\Xi\right]}{\Phi(\beta-\delta)}\right\}^{\frac{p+1}{2}},\\ \times K_{p+1}\left(2\sqrt{\frac{\lambda_{\mathrm{RD}_n}\gamma_{th}(\beta-\delta)\left[\gamma_{th}\vartheta_1\vartheta_3+\Xi\right]}{\Phi\Psi}}\right),\end{aligned} \quad (33)$$

$$\begin{aligned}Q_{33} = 2\sum_{q=1}^{N-1}(-1)^{q+1}\widetilde{\sum}\sum_{k=0}^{m_s-1}\sum_{p=0}^{k}\binom{k}{p}\times\frac{\alpha\zeta(k)\lambda_{\mathrm{RD}_n}}{\lambda_{n,q}^{\mathrm{sum}}+\lambda_{\mathrm{RD}_n}}\\ \times\frac{\left[\gamma_{th}\left(\mu_{\mathrm{SR}}^2\Psi+1\right)\right]^{k-p}}{\Psi^{k+1}}\\ \times\exp\left(-\frac{(\beta-\delta)\gamma_{th}\vartheta_1}{\Psi}-\frac{\left(\lambda_{n,q}^{\mathrm{sum}}+\lambda_{\mathrm{RD}_n}\right)\gamma_{th}\vartheta_3}{\Phi}\right)\\ \times\left\{\frac{\left(\lambda_{n,q}^{\mathrm{sum}}+\lambda_{\mathrm{RD}_n}\right)\gamma_{th}\Psi\left[\gamma_{th}\vartheta_1\vartheta_3+\Xi\right]}{\Phi(\beta-\delta)}\right\}^{\frac{p+1}{2}}\\ \times K_{p+1}\left(2\sqrt{\frac{\left(\lambda_{n,q}^{\mathrm{sum}}+\lambda_{\mathrm{RD}_n}\right)\gamma_{th}(\beta-\delta)\left[\gamma_{th}\vartheta_1\vartheta_3+\Xi\right]}{\Phi\Psi}}\right)\end{aligned}$$

$$\widetilde{\lambda}^{\mathrm{sum}} \triangleq \lambda_{n,q}^{\mathrm{sum}}+\lambda_{\mathrm{RD_n}}. \quad (34)$$

*Proof:* See Appendix A. ■

**Theorem 1:** In AF relaying system with i.n.i.d. Raleigh fading channel, the exact closed-form expression of OP can be expressed as

$$\begin{aligned}\mathrm{OP}^{\mathrm{AF}} = 1-2\sum_{n=1}^{N}\sum_{q=1}^{N-1}(-1)^{q+1}\widetilde{\sum}\sum_{k=0}^{m_s-1}\sum_{p=0}^{k}\binom{k}{p}\\ \times\frac{\alpha\zeta(k)[\gamma_{th}\vartheta_1]^{k-p}}{\Psi^{k+1}}\left\{\frac{\gamma_{th}\Psi\left[\gamma_{th}\vartheta_1\vartheta_3+\Xi\right]}{\Phi(\beta-\delta)}\right\}^{\frac{p+1}{2}}\\ \times\exp\left(-\frac{(\beta-\delta)\gamma_{th}\vartheta_1}{\Psi}\right)\times\left\{\pi_1\times\pi_2-\pi_3\times\pi_4\right\},\end{aligned} \quad (35)$$

where

$$\pi_1 \triangleq \left(\lambda_{\mathrm{RD}_n}\right)^{\frac{p+1}{2}} \exp\left(-\frac{\lambda_{\mathrm{RD}_n}\gamma_{th}\vartheta_3}{\Phi}\right), \tag{36}$$

$$\pi_2 \triangleq K_{p+1}\left(2\sqrt{\frac{\lambda_{\mathrm{RD}_n}\gamma_{th}\left(\beta-\delta\right)\left[\gamma_{th}\vartheta_1\vartheta_3+\Xi\right]}{\Phi\Psi}}\right), \tag{37}$$

$$\pi_3 \triangleq \lambda_{\mathrm{RD}_n}\left(\widetilde{\lambda}^{\mathrm{sum}}\right)^{\frac{p-1}{2}} \exp\left(-\frac{\widetilde{\lambda}^{\mathrm{sum}}\gamma_{th}\vartheta_3}{\Phi}\right), \tag{38}$$

$$\pi_4 \triangleq K_{p+1}\left(2\sqrt{\frac{\widetilde{\lambda}^{\mathrm{sum}}\gamma_{th}\left(\beta-\delta\right)\left[\gamma_{th}\vartheta_1\vartheta_3+\Xi\right]}{\Phi\Psi}}\right). \tag{39}$$

*Proof:* By substituting (29), (30) and (62) into (25), we obtain the exact closed-form of $\mathrm{OP}^{\mathrm{AF}}$ as in (35). ■

The outage probability in (35) is upper bounded by one and includes the effects of the friendly jammer, eavesdropper, and relay. We note that the secrecy outage probability is nontrivial to obtain for the considered system model and should be a potential topic for further work.

*2) Intercept Probability* (IP) *Analysis:* Destinations can be intercepted if eavesdroppers can successfully decode signals, i.e., $\gamma_{\mathrm{E}}^{l} \geq \gamma_{th}$ ($l \in \{\mathrm{AF}, \mathrm{DF}\}$). Therefore, the IP can be defined as [56]–[58]

$$\mathrm{IP}^{l} = \Pr\left(\gamma_{\mathrm{E}}^{l} \geq \gamma_{th}\right) = 1 - \Pr\left(\gamma_{\mathrm{E}}^{l} < \gamma_{th}\right) \tag{40}$$

Based on (21), the $\mathrm{IP}^{\mathrm{AF}}$ can be given by

$$\mathrm{IP}^{\mathrm{AF}} = 1 - \sum_{m=1}^{M} \underbrace{\Pr\left(\gamma_{\mathrm{RE}_m}^{\mathrm{N-COL}} > Z_m, \frac{\Psi\Phi\gamma_{\mathrm{SR}}\gamma_{\mathrm{RE}_m}^{\mathrm{N-COL}}}{\pi_5} < \gamma_{th}\right)}_{\mathrm{P}}, \tag{41}$$

where

$$Z_m \triangleq \max_{a=1,2,\ldots,M, a\neq m}\left(\gamma_{\mathrm{RD}_a}\right) \tag{42}$$

$$\pi_5 \triangleq \gamma_{\mathrm{RE}_m}^{\mathrm{N-COL}}\Phi\vartheta_1 + \gamma_{\mathrm{SR}}\Psi\vartheta_4 + \gamma_{\mathrm{JE}_m}\Theta\vartheta_1 + \Lambda. \tag{43}$$

*Lemma 3:* Based on (26) and (27), the CDF and PDF of $Z_m$ can be respectively given as

$$F_{Z_m}(x) = 1 + \sum_{a=1}^{M-1}\left(-1\right)^{a}\widetilde{\sum}^{M} \exp\left(-\lambda_{m,a}^{\mathrm{sum}}x\right), \tag{44}$$

$$f_{Z_m}(x) = \sum_{a=1}^{M-1}\left(-1\right)^{a+1}\widetilde{\sum}^{M} \lambda_{m,a}^{\mathrm{sum}} \exp\left(-\lambda_{m,a}^{\mathrm{sum}}x\right), \tag{45}$$

where $\lambda_{m,a}^{\mathrm{sum}} = \sum_{i=1}^{a}\lambda_{\mathrm{RE}_{j_i}}$, $\widetilde{\sum}^{M} \triangleq \sum_{\substack{j_1=\cdots=j_a=1,\\ j_1<\cdots<j_a,\\ j_1,\ldots,j_a\neq m}}^{M}$.

**Theorem 2:** In AF relaying system with i.n.i.d. Raleigh fading channel, the analysis expression of IP can be expressed as:

$$\begin{aligned}\mathrm{IP}^{\mathrm{AF}} = {} & 2\sum_{m=1}^{M}\sum_{a=1}^{M-1}\left(-1\right)^{a+1}\widetilde{\sum}^{M}\sum_{k=0}^{m_s-1}\sum_{p=0}^{k}\binom{k}{p} \\ & \times \frac{\alpha\zeta(k)\lambda_{\mathrm{JE}_m}\left[\gamma_{th}\vartheta_1\right]^{k-p}}{\Psi^{k-p/2+1/2}\left[\Phi\left(\beta-\delta\right)\right]^{\frac{p+1}{2}}} \exp\left(-\frac{\left(\beta-\delta\right)\gamma_{th}\vartheta_1}{\Psi}\right) \\ & \times \int_0^{\infty}\left\{\begin{array}{l} \left[h_1(x)\right]^{\frac{p+1}{2}} \exp\left(-\frac{g_1(x)}{\Phi}-\lambda_{\mathrm{JE}_m}x\right) \\ \times K_{p+1}\left(2\sqrt{\frac{h_1(x)(\beta-\delta)}{\Phi\Psi}}\right) \\ -\frac{\lambda_{\mathrm{RE}_m}\left[h_2(x)\right]^{\frac{p+1}{2}}}{\lambda_{n,q}^{\mathrm{sum}}+\lambda_{\mathrm{RE}_m}} \exp\left(-\frac{g_2(x)}{\Phi}-\lambda_{\mathrm{JE}_m}x\right) \\ \times K_{p+1}\left(2\sqrt{\frac{h_2(x)(\beta-\delta)}{\Phi\Psi}}\right) \end{array}\right\} dx.\end{aligned} \tag{46}$$

*Proof:* See Appendix B. ■

*B.* DF Relaying Protocol

*1)* OP Analysis: Based on (16) and (24), the $\mathrm{OP}^{\mathrm{DF}}$ can be expressed by

$$\begin{aligned}\mathrm{OP}^{\mathrm{DF}} &= \sum_{n=1}^{N}\Pr\left(\gamma_{\mathrm{RD}_n} = \max_{q=1,2,\ldots,N}\left(\gamma_{\mathrm{RD}_q}\right), \gamma_{\mathrm{D}_n}^{\mathrm{DF}} < \gamma_{th}\right) \\ &= 1 - \sum_{n=1}^{N}\Pr\left(\gamma_{\mathrm{RD}_n} > Z_n, \gamma_{\mathrm{R}} \geq \gamma_{th}, \gamma_{\mathrm{RD}_n} \geq \gamma_{th}\right) \\ &= 1 - \underbrace{\left\{1 - \Pr\left(\gamma_{\mathrm{R}} < \gamma_{th}\right)\right\}}_{\mathrm{OP}_1} \\ &\quad \times \underbrace{\left\{1 - \sum_{n=1}^{N}\Pr\left(\gamma_{\mathrm{RD}_n} > Z_n, \gamma_{\mathrm{RD}_n} < \gamma_{th}\right)\right\}}_{\mathrm{OP}_2}.\end{aligned} \tag{47}$$

**Theorem 3:** By using the same approach as (55), for DF relaying system with i.n.i.d. Raleigh fading channel, the closed-form expression of OP can be expressed as:

$$\begin{aligned}\mathrm{OP}^{\mathrm{DF}} = {} & 1 - \alpha\sum_{k=0}^{m_s-1}\sum_{p=0}^{k}\frac{\zeta(k)k!}{p!(\beta-\delta)^{(k+1-p)}} \\ & \times \left[\frac{\gamma_{th}\vartheta_1}{\Psi}\right]^{p} \exp\left(-\frac{\gamma_{th}\vartheta_1\left(\beta-\delta\right)}{\Psi}\right) \\ & \times \left\{1 - \sum_{n=1}^{N}\sum_{q=1}^{N-1}\left(-1\right)^{q+1}\right. \\ & \left.\times \widetilde{\sum}\left\{\begin{array}{l}\frac{\lambda_{n,q}^{\mathrm{sum}}}{\widetilde{\lambda}^{\mathrm{sum}}} - \exp\left(-\frac{\lambda_{\mathrm{RD}_n}\gamma_{th}\vartheta_3}{\Phi}\right) \\ +\frac{\lambda_{\mathrm{RD}_n}}{\widetilde{\lambda}^{\mathrm{sum}}} \exp\left(-\frac{\widetilde{\lambda}^{\mathrm{sum}}\gamma_{th}\vartheta_3}{\Phi}\right)\end{array}\right\}\right\}.\end{aligned} \tag{48}$$

*Proof:* See Appendix C. ■

*2)* IP Analysis: From (22) and (40), the $\mathrm{IP}^{\mathrm{DF}}$ can be expressed as

$$\mathrm{IP}^{\mathrm{DF}} = \sum_{m=1}^{M}\Pr\left(\gamma_{\mathrm{RE}_m}^{\mathrm{N-COL}} = \max_{a=1,\ldots,M}\left\{\gamma_{\mathrm{RE}_a}\right\}, \gamma_{\mathrm{E}_m}^{\mathrm{DF,N-COL}} \geq \gamma_{th}\right) \tag{49}$$

$$= \sum_{m=1}^{M} \Pr\left(\gamma_{\mathrm{RE}_m}^{\mathrm{N-COL}} > Z_m, \gamma_{\mathrm{R}} \geq \gamma_{th}, \frac{\Phi\gamma_{\mathrm{RE}_m}^{\mathrm{N-COL}}}{\vartheta_4} \geq \gamma_{th}\right)$$

$$= \left\{1 - F_{\gamma_{\mathrm{R}}}(\gamma_{th})\right\}\left\{1 - \sum_{m=1}^{M} \mathrm{W}\right\},$$

where $\mathrm{W} \triangleq \Pr\left(\gamma_{\mathrm{RE}_m}^{\mathrm{N-COL}} > Z_m, \Phi\gamma_{\mathrm{RE}_m}^{\mathrm{N-COL}} < \frac{\gamma_{th}\vartheta_4}{\Phi}\right)$.

**Theorem 4:** For DF relaying system with i.n.i.d. Raleigh fading channel, the closed-form expression of IP can be expressed as:

$$\mathrm{IP}^{\mathrm{DF}} = \alpha \sum_{k=0}^{m_s-1} \sum_{p=0}^{k} \frac{\zeta(k)k!}{p!(\beta-\delta)^{(k+1-p)}} \times \left[\frac{\gamma_{th}\vartheta_1}{\Psi}\right]^p \times \exp\left(-\frac{\gamma_{th}\vartheta_1(\beta-\delta)}{\Psi}\right) \sum_{m=1}^{M} \sum_{a=1}^{M-1} (-1)^{a+1} \times \widetilde{\sum}^{M} \left\{ \begin{array}{l} \frac{\lambda_{\mathrm{JE}_m}\Phi}{\lambda_{\mathrm{RE}_m}\gamma_{th}\Theta+\lambda_{\mathrm{JE}_m}\Phi} \\ \times \exp\left(-\frac{\lambda_{\mathrm{RE}_m}\gamma_{th}\left(\Theta\mu_{\mathrm{JE}_m}^2+\Phi\mu_{\mathrm{RE}_m}^2+1\right)}{\Phi}\right) \\ -\frac{\lambda_{m,a}^{\mathrm{sum}}\lambda_{\mathrm{JE}_m}\Phi}{\widetilde{\lambda}_{\mathrm{RE}}\left[\widetilde{\lambda}_{\mathrm{RE}}\gamma_{th}\Theta+\Phi\lambda_{\mathrm{JE}_m}\right]} \\ \times \exp\left(-\frac{\widetilde{\lambda}_{\mathrm{RE}}\gamma_{th}\left(\Theta\mu_{\mathrm{JE}_m}^2+\Phi\mu_{\mathrm{RE}_m}^2+1\right)}{\Phi}\right) \end{array} \right\}, \quad (50)$$

where $\widetilde{\lambda}_{\mathrm{RE}} \triangleq \lambda_{m,a}^{\mathrm{sum}} + \lambda_{\mathrm{RE_m}}$.

*Proof:* See Appendix D. ∎

Both the obtained analytical expressions of the IP and OP are independent of small-scale fading coefficients, and therefore applied for a long period of time. These system performance metrics are only updated as the channel statistics change. We notice that an asymptotic analysis is challenging and left for future work since the transmit power of the satellite and the selected relay is independent of each other.

## IV. Simulation Results

In this section, numerical simulations are provided to confirm the validity of the theoretical analysis and the effects of system parameters on the performance of the proposed satellite-terrestrial relay networks. In this simulation, the channel between satellite and relay is Shadowed-Rician, while the channels between relay R to ground users are subject to non-identical Rayleigh channels. Moreover, all simulations are performed through $10^6$ independent realizations to obtain the OP and IP values. Unless otherwise stated, the settings of simulation parameters are listed in Table I. For ease of notation and clear observation, we denote methods $(m_s, b, \Omega_s) = (1, 0.065, 0.0005)$ and $(m_s, b, \Omega_s) = (5, 0.25, 0.3)$ as proposed scheme 1 (PS1) and proposed scheme 2 (PS2), respectively.

In Figs. 2 and 3, we plots the OP and IP as functions of $\Psi$ (dB), where fading severity parameter $m_s$, average power of light-of-sight (LoS) $\Omega_s$, and multi-path components $2b$, are set as 1, 0.065, and 0.0005, respectively. As shown in Fig. 2, when the $\Psi$ value increases from $0 \to 50$ dB, the better outage performance can be obtained. For instance, the OP values of PS1 with $N = 1$ are 0.9999, 0.6782, and 0.2159 corresponding to $\Psi$ equals 10, 20, and 39 dB, respectively. Because $\Psi$ is a function of $P_{\mathrm{S}}/N_0$, whereas $P_{\mathrm{S}}$ and $N_0$ are the satellite transmit power and AWGN. Therefore, a higher $\Psi$ value means that more power allocated for satellite, which enhances the probability of successfully decode signals. It also can be observed from Fig. 2 that the outage performance of PS2-based schemes outperforms the PS1-based schemes. For instance, at $\Psi$ equals 30 dB, the OP value of PS1-CEEs=0.15, PS1-perfect CSI, PS2-CEEs=0.15, and PS2-perfect CSI are 0.2159, 0.1312, 0.0793, and 0.0138, respectively. On more interesting observation from Fig. 2 is that the outage performance is significantly improved with a higher number of destinations, i.e., $N$ from 1 to 3. This is because we have more chances to select a better channel from $\mathrm{R} \to \mathrm{D_n}$, which improves the network performance. In Fig. 3, the higher the $\Psi$ value is, the better intercept performance can be obtained. For example, for PS2-M=3 scheme, the IP values are 0.0119, 0.2603, and 0.6493 corresponding to $\Psi$ equals 0, 5, 10 dB, respectively. Moreover, the increasing of the number of destinations also improves the IP since the eavesdroppers have more chances to obtain a better channel from $\mathrm{R} \to \mathrm{E_m}$. For example, at $\Psi$ equals 10 dB, the IP of PS1-CEEs=0.15, PS1-perfect CSI, PS2-CEEs=0.15, and PS2-perfect CSI are 0.000834, 0.0756, 0.0452, and 0.6493, respectively.

In Figs. 4 and 5, the security-reliability trade-off is investigated for PS1 and PS2 schemes. It is clear to see from Fig. 4 and 5 that for any specific IP the OP of the PS1 (or PS2) with N = M = 1 superior than PS1 (or PS2) with N = M = 2. For instance, when OP equals 0.4248, the OP of PS1 (or PS2 ) with N = M = 1 is 0.5489 (or 0.1159), while the OP of PS1 (or PS2 ) with N = M = 2 imposes 0.6782 (or 0.2598). When the OP is small, e.g., OP from $10^{-10} \to 10^{-4}$ in Fig. 4, the IP gap between PS1 with N = M = 1 and PS1 with N = M = 3 is neglect-able. While OP is large enough, e.g., OP from $10^{-4} \to 10^{0}$ in Fig. 4, the IP gap between PS1 with N = M = 1 and PS1 with N = M = 3 is significantly increasing.

Figs. 6 and 7 illustrate OP and IP as functions of $\Psi$ (dB) for perfect and imperfect CS. First, it can be seen from Fig. 6 that the outage performance of the PS1-based schemes is worse than that of PS2-based schemes as mentioned in Fig. 2. Specifically, at $\Psi$ equals 30, the OP is 0.4496, 0.0271, 0.0882, and 0.0056 corresponding to PS1-CEEs=0.15, PS1-perfect CSI, PS2-CEEs=0.15, and PS1-perfect CSI, respectively. Second, we also see that the outage performance of the perfect CSI schemes superior than that of the imperfect CSI ones. For instance, at $\Psi$ = 50 dB, the OP of PS1-CEEs=0.15 and PS1-perfect CSI impose 0.4357 and 0.0847, respectively. Moreover, it can be seen from Fig. 7 that the intercept performance of the perfect CSI-based scheme is better than that of imperfect CSI-based ones. Specifically, at $\Psi$ = 10 dB, the IP values of the PS1-CEEs=0.15 and PS1-perfect CSI are 0.0423 and 0.0756, respectively. One more interesting point can be observed from Fig. 7 that the gap between perfect and imperfect schemes for PS2 is smaller than that compared to that of PS1 scheme.

In Figs. 8 and 9, we plots OP and IP as functions of channel estimation error for both PS1- and PS2-based schemes. It can be seen from Fig. 8 that the higher the CEEs is, the worse the OP can be obtained. Specifically, when CEEs equals 0.2, the OP of PS2-$\Phi = 10$ dB, PS2-$\phi = 5$ dB, PS1-$\Phi = 10$ dB, and PS1-$\Phi = 5$ dB are 0.182, 0.2578, 0.3339, and 0.3713, respectively. This is expected since the SNR at the relay or

TABLE I
SIMULATION PARAMETERS

| Symbol | Parameter name | Fixed value | Varying range |
|---|---|---|---|
| $C_{th}$ | Source rate | 0.5 bps/Hz | none |
| $\Psi$ | Transmit-power-to-noise-ratio of source | 20 dB | 0 to 50 (dB) |
| $\Phi$ | Transmit-power-to-noise-ratio of relay | 5; 10 dB | -5 to 20 (dB) |
| $\Theta$ | Transmit-power-to-noise-ratio of jammer | 1 dB | -5 to 10 (dB) |
| $N$ | No. of destination nodes | 1; 2; 3 | none |
| $M$ | No. of eavesdropper nodes | 1; 2; 3 | none |
| $\mu_{\mathrm{SR}}$ | CEE of S-R link | 0; 0.15; 0.25; 0.5 | 0 to 0.5 |
| $\mu_{\mathrm{RD_n}}$ | CEE of R-D link | 0; 0.15; 0.25; 0.5 | 0 to 0.5 |
| $\mu_{\mathrm{RE_m}}$ | CEE of R-E link | 0; 0.15; 0.25; 0.5 | 0 to 0.5 |
| $\mu_{\mathrm{JE_m}}$ | CEE of J-E link | 0; 0.15; 0.25; 0.5 | 0 to 0.5 |

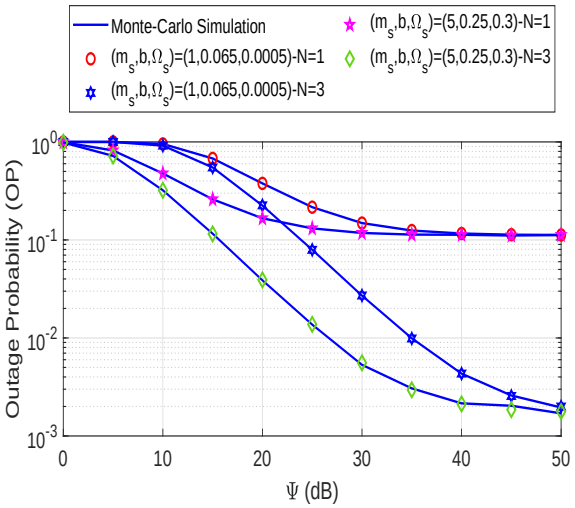


Fig. 2. OP versus Ψ for DF-based relaying scheme.

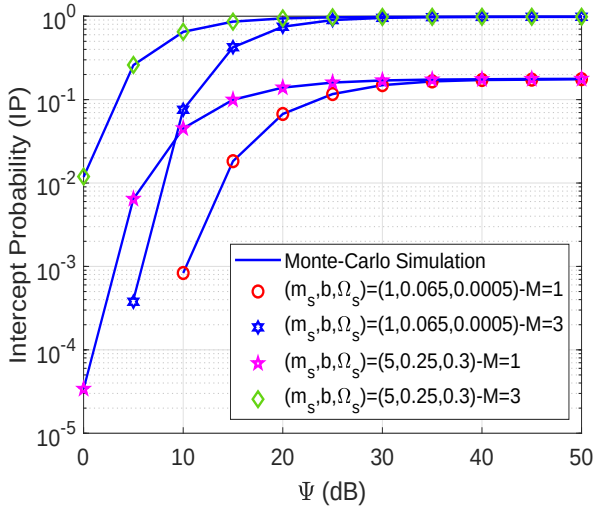


Fig. 3. IP versus Ψ for DF-based relaying scheme.

destination is deteriorated with a higher CEEs value as shown in equations (11). Furthermore, it can be seen from Fig. 9 that when CEEs is less than 0.1, the intercept performance of PS1 with Ψ = 10 dB outperforms PS1 with Ψ = 5 dB. For instance, at CEEs = 0.05, the IP values of PS1 with Ψ = 10 dB and PS1 with Ψ = 5 dB are 0.8517 and 0.7886, respectively. Nevertheless, when CEEs is larger than 0.1, the IP of PS1 with Ψ = 10 dB deteriorates compared to that of PS1 with Ψ = 5 dB. Specifically, at CEEs = 0.5, the the IP values of PS1 with Ψ = 10 dB and PS1 with Ψ = 5 dB impose 0.0846 and 0.0626, respectively.

In Figs. 10 and 11, the influences of the relay transmit power on the OP and IP are investigated for both perfect and imperfect CSI. It can be observed from Fig. 10 that the outage performance of all schemes is significantly improved with the increase of Φ values. It is expected since the Φ can be defined as $\frac{P_{\mathrm{R}}}{N_0}$; thus, a higher Φ value means that more transmit power is allocated for relay R. Therefore, the higher the Φ value is, the better OP can be obtained. Specifically, when Φ equals 5 dB, the OP of PS1 with perfect CSI, PS1-CEEs = 0.5, PS2-CEEs = 0.5, and PS2 with perfect CSI are 0.2016, 0.0741, 0.0402, 0.0355, respectively. In Fig. 11, the IP is investigated as a function of Φ (dB). It can be easy to see from Fig. 11 that the intercept performance of the PS2 schemes are superior than PS1 schemes when Φ ¡ 4 dB. However, when Φ > 4 dB, the IP of the PS2 is worse than that of PS1 ones. For instance, at Φ = 10 (dB), the IP of the PS1 with perfect CSI, PS1-CEEs = 0.5, PS2-CEEs = 0.5, and PS2 with perfect CSI are 0.7925, 0.9242, 0.9525, and 0.9639, respectively.

## V. Conclusion and Future Directions

In this paper, we have investigated the security and reliability trade-off of a satellite AF relay network, including one satellite, one relay, multiple destinations in the presence of multiple eavesdroppers. In particular, a jammer has been deployed to create artificial noise that reduces the impact of eavesdroppers on the system performance. In this context, the closed-form analyses of OP and IP were derived over Shadowed Rician and non-identical Rayleigh fading for the first and second hop, respectively. Notably, these analyses have been corroborated via simulation results. Based on the obtained OP and IP results, we studied the security-reliability trade-off for the proposed system and recommended suitable system parameters satisfying requirements in real scenarios. Specifically, the values of satellite transmit power, relay transmit power, and the number of destinations can be chosen appropriately to worsen the influences of eavesdroppers.

Our findings revealed that different from the conventional satellite-terrestrial networks, increasing the transmit power at source and relay is always helpful for the system. In the considered STN, there exist optimal values of both the transmit power at source and relay that compromise the security and reliability of the system. Moreover, the impact of channel

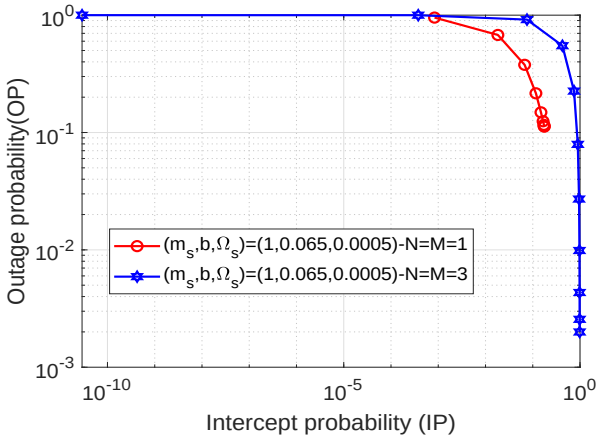


Fig. 4. OP versus IP for DF-based relaying scheme, where $(m_s, b, \Omega_s) = (1, 0.065, 0.0005)$.

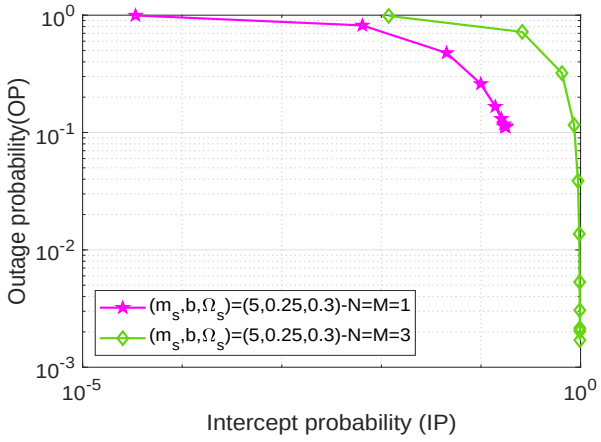


Fig. 5. OP versus IP for DF-based relaying scheme, where $(m_s, b, \Omega_s) = (5, 0.25, 0.3)$.

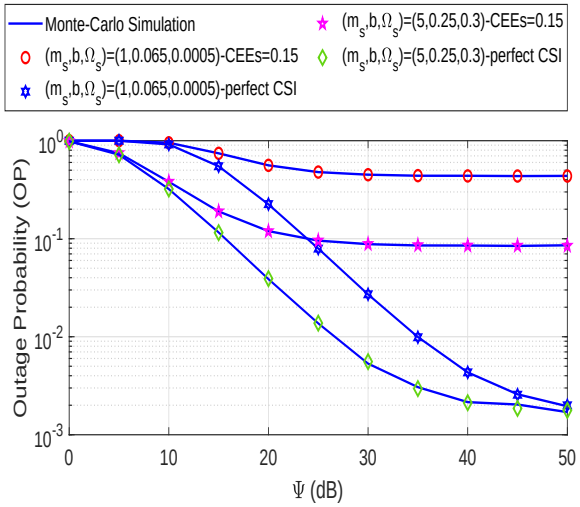


Fig. 6. OP versus $\Psi$ for DF-based relaying scheme with perfect and imperfect CSI.

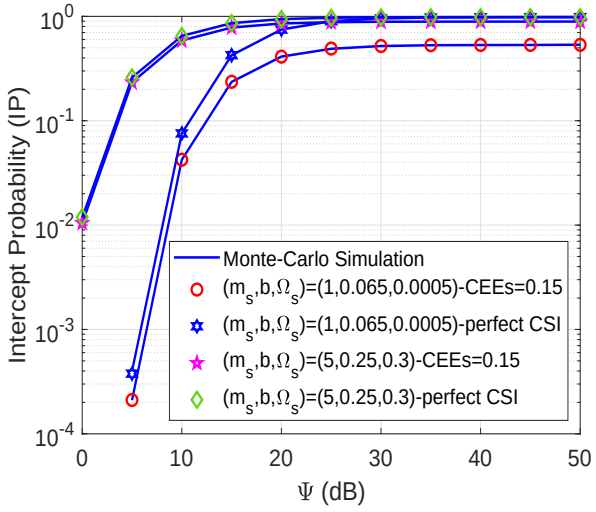


Fig. 7. IP versus $\Psi$ for DF-based relaying scheme with perfect and imperfect CSI.

estimation error on the system performance is not consistently harmful. Numerical results showed that channel estimation error is useful for scaling down the intercept probability. We can either employ multiple relays and/or IRS like [59], [60] to enhance the system performance.

## Appendix A: Proof of Lemma 2

From (25), Q can be calculated by

$$\begin{aligned} Q &= \Pr\left(\gamma_{\mathrm{RD}_n} > Z_n, \frac{\Psi\Phi\gamma_{\mathrm{SR}}\gamma_{\mathrm{RD}_n}}{\gamma_{\mathrm{RD}_n}\Phi\vartheta_1 + \gamma_{\mathrm{SR}}\Psi\vartheta_3 + \Xi} < \gamma_{th}\right) \\ &= \Pr\left(\gamma_{\mathrm{RD}_n} > Z_n, \gamma_{\mathrm{RD}_n}\Phi\varrho_1 < \gamma_{th}\left[\gamma_{\mathrm{SR}}\Psi\vartheta_3 + \Xi\right]\right) \\ &= \begin{cases} \Pr\left(\gamma_{\mathrm{RD}_n} > Z_n\right), & \text{if } \varrho_1 \le 0 \\ \Pr\left(\gamma_{\mathrm{RD}_n} > Z_n, \gamma_{\mathrm{RD}_n} < \frac{\gamma_{th}\left[\gamma_{\mathrm{SR}}\Psi\vartheta_3+\Xi\right]}{\Phi\varrho_1}\right), & \text{if } \varrho_1 > 0 \end{cases} \\ &= \underbrace{\Pr\left(\gamma_{\mathrm{RD}_n} > Z_n\right)}_{Q_1}\underbrace{\Pr\left(\varrho_1 \le 0\right)}_{Q_2} \end{aligned}$$

$$+ \underbrace{\int_{\frac{\gamma_{th}\vartheta_1}{\Psi}}^{\infty} \underbrace{\Pr\left(Z_n < \gamma_{\mathrm{RD}_n} < \frac{\gamma_{th}\left[x\Psi\vartheta_3 + \Xi\right]}{\Phi\left[x\Psi - \gamma_{th}\vartheta_1\right]}\right)}_{\bar{Q}_3} \times f_{\gamma_{\mathrm{SR}}}(x)dx}_{Q_3}, \tag{51}$$

where $\varrho_1 \triangleq \Psi\gamma_{\mathrm{SR}} - \gamma_{th}\vartheta_1$. Based on (51), $Q_1$ can be calculated as

$$\begin{aligned} Q_1 &= \Pr\left(\gamma_{\mathrm{RD}_n} > Z_n\right) = \int_0^{\infty}\int_z^{\infty} f_{\gamma_{\mathrm{RD}_n}}(y) \times f_{Z_n}(z)dydz \\ &= \int_0^{\infty} \exp\left(-\lambda_{\mathrm{RD}_n} z\right) \times f_{Z_n}(z)dz. \end{aligned} \tag{52}$$

By applying (27), $Q_1$ can be obtained as in (29). From (51), $Q_2$ can be given by

$$\begin{aligned} Q_2 &= \Pr\left(\Psi\gamma_{\mathrm{SR}} - \gamma_{th}\vartheta_1 \le 0\right) \\ &= \Pr\left(\gamma_{\mathrm{SR}} \le \frac{\gamma_{th}\vartheta_1}{\Psi}\right) = F_{\gamma_{\mathrm{SR}}}\left(\frac{\gamma_{th}\vartheta_1}{\Psi}\right), \end{aligned} \tag{53}$$

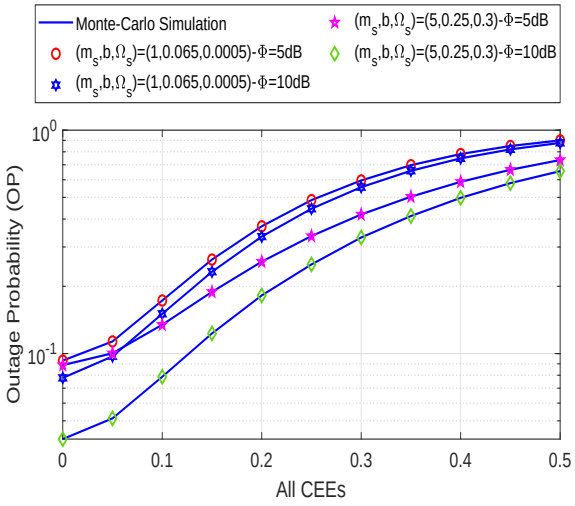


Fig. 8. OP versus CEEs for DF-based relaying scheme.

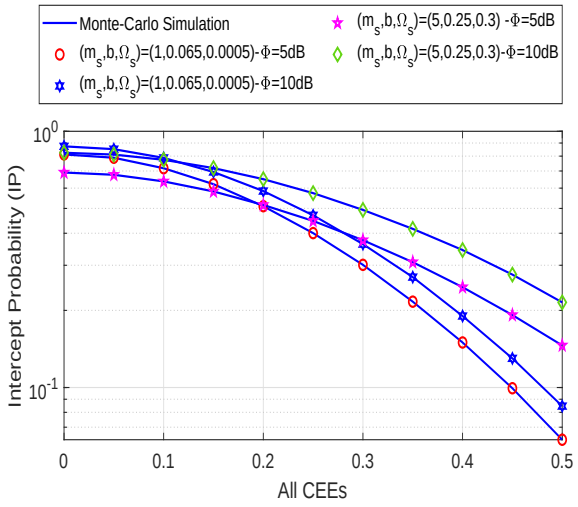


Fig. 9. IP versus CEEs for DF-based relaying scheme.

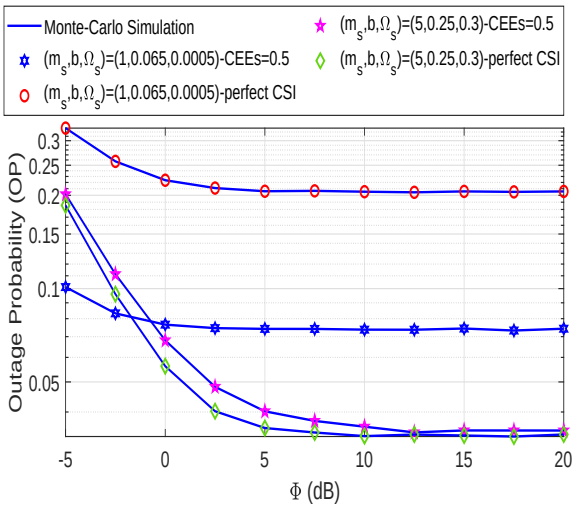


Fig. 10. OP versus Φ (dB) for AF-based relaying scheme.

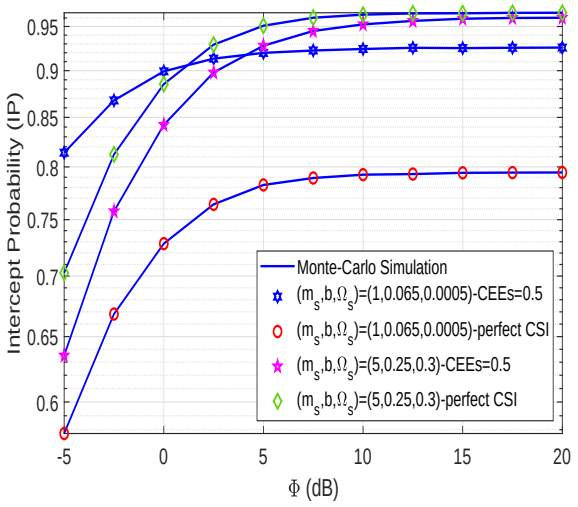


Fig. 11. IP versus Φ (dB) for AF-based relaying scheme.

By applying (5), the closed-form expression of $Q_2$ can be presented as in (30). Next, from (51), $\tilde{Q}_3$ can be calculated as

$$\begin{aligned}
&\tilde{Q}_3 \\
&= \Pr\left(Z_n < \gamma_{\mathrm{RD}_n} < \frac{\gamma_{th}\left[x\Psi\vartheta_3+\Xi\right]}{\Phi\left[x\Psi-\gamma_{th}\vartheta_1\right]}\right) \\
&= \int_0^{\frac{\gamma_{th}\left[x\Psi\vartheta_3+\Xi\right]}{\Phi\left[x\Psi-\gamma_{th}\vartheta_1\right]}} \int_z^{\frac{\gamma_{th}\left[x\Psi\vartheta_3+\Xi\right]}{\Phi\left[x\Psi-\gamma_{th}\vartheta_1\right]}} f_{\gamma_{\mathrm{RD}_n}}(y) f_{Z_n}(z) dy dz \\
&= \int_0^{\frac{\gamma_{th}\left[x\Psi\vartheta_3+\Xi\right]}{\Phi\left[x\Psi-\gamma_{th}\vartheta_1\right]}} f_{Z_n}(z)\exp(\varrho_2) dz, \qquad (54)
\end{aligned}$$

where $\varrho_2 \triangleq -\lambda_{\mathrm{RD}_n} z - \frac{\lambda_{\mathrm{RD}_n}\gamma_{th}\left[x\Psi\vartheta_3+\Xi\right]}{\Phi\left[x\Psi-\gamma_{th}\vartheta_1\right]}$. By substituting (27) into (54), $\tilde{Q}_3$ can be reformulated as

$$\begin{aligned}
&\tilde{Q}_3 \\
&= \int_0^{\frac{\gamma_{th}\left[x\Psi\vartheta_3+\Xi\right]}{\Phi\left[x\Psi-\gamma_{th}\left(\mu_{\mathrm{SR}}\Psi+1\right)\right]}} \left\{ \begin{array}{l} \sum_{q=1}^{N-1} (-1)^{q+1} \widetilde{\sum} \lambda_{n,q}^{\mathrm{sum}} \exp\left(-\lambda_{n,q}^{\mathrm{sum}} z\right) \\ \times \left[ \exp\left(-\lambda_{\mathrm{RD}_n} z\right) \right. \\ \left. - \exp\left(-\frac{\lambda_{\mathrm{RD}_n}\gamma_{th}\left[x\Psi\vartheta_3+\Xi\right]}{\Phi\left[x\Psi-\gamma_{th}\vartheta_1\right]}\right) \right] \end{array} \right\} dz \\
&= \sum_{q=1}^{N-1} (-1)^{q+1} \widetilde{\sum} \frac{\lambda_{n,q}^{\mathrm{sum}}}{\widetilde{\lambda}^{\mathrm{sum}}} \left[ 1 - \exp\left( -\frac{\widetilde{\lambda}^{\mathrm{sum}}\gamma_{th}\left[x\Psi\vartheta_3+\Xi\right]}{\Phi\left[x\Psi-\gamma_{th}\vartheta_1\right]} \right) \right] \\
&\quad - \sum_{q=1}^{N-1} (-1)^{q+1} \widetilde{\sum} \exp\left( -\frac{\lambda_{\mathrm{RD}_n}\gamma_{th}\left[x\Psi\vartheta_3+\Xi\right]}{\Phi\left[x\Psi-\gamma_{th}\vartheta_1\right]} \right)
\end{aligned}$$

$$\times\left[1-\exp\left(-\frac{\lambda_{n,q}^{\mathrm{sum}}\gamma_{th}\left[x\Psi\vartheta_3+\Xi\right]}{\Phi\left[x\Psi-\gamma_{th}\vartheta_1\right]}\right)\right]$$
$$=\sum_{q=1}^{N-1}(-1)^{q+1}\widetilde{\sum}\left\{\begin{array}{l}\frac{\lambda_{n,q}^{\mathrm{sum}}}{\widetilde{\lambda}^{\mathrm{sum}}}-\exp\left(-\frac{\lambda_{\mathrm{RD}_n}\gamma_{th}[x\Psi\vartheta_3+\Xi]}{\Phi[x\Psi-\gamma_{th}\vartheta_1]}\right)\\+\frac{\lambda_{\mathrm{RD}_n}}{\widetilde{\lambda}^{\mathrm{sum}}}\exp\left(-\frac{\widetilde{\lambda}^{\mathrm{sum}}\gamma_{th}[x\Psi\vartheta_3+\Xi]}{\Phi[x\Psi-\gamma_{th}\vartheta_1]}\right)\end{array}\right\}. \tag{55}$$

From (4), (51) and (55), $Q_3$ can be calculated as

$$Q_3=\sum_{q=1}^{N-1}(-1)^{q+1}\widetilde{\sum}\times\int_{\frac{\gamma_{th}\vartheta_1}{\Psi}}^{\infty}\left\{\begin{array}{l}\frac{\lambda_{n,q}^{\mathrm{sum}}}{\widetilde{\lambda}^{\mathrm{sum}}}-\exp\left(-\frac{\lambda_{\mathrm{RD}_n}\gamma_{th}[x\Psi\vartheta_3+\Xi]}{\Phi[x\Psi-\gamma_{th}\vartheta_1]}\right)\\+\frac{\lambda_{\mathrm{RD}_n}}{\widetilde{\lambda}^{\mathrm{sum}}}\exp\left(-\frac{\widetilde{\lambda}^{\mathrm{sum}}\gamma_{th}[x\Psi\vartheta_3+\Xi]}{\Phi[x\Psi-\gamma_{th}\vartheta_1]}\right)\end{array}\right\}\times f_{\gamma_{\mathrm{SR}}}(x)dx$$
$$=\underbrace{\sum_{q=1}^{N-1}(-1)^{q+1}\widetilde{\sum}\frac{\lambda_{n,q}^{\mathrm{sum}}}{\widetilde{\lambda}^{\mathrm{sum}}}\int_{\frac{\gamma_{th}\vartheta_1}{\Psi}}^{\infty}f_{\gamma_{\mathrm{SR}}}(x)dx}_{Q_{31}}-Q_{32}+Q_{33}, \tag{56}$$

where

$$Q_{32}\triangleq\sum_{q=1}^{N-1}(-1)^{q+1}\widetilde{\sum}\sum_{k=0}^{m_s-1}\alpha\zeta(k)\int_{\frac{\gamma_{th}\vartheta_1}{\Psi}}^{\infty}x^k\exp\left(-\frac{\lambda_{\mathrm{RD}_n}\gamma_{th}\left[x\Psi\vartheta_3+\Xi\right]}{\Phi\left[x\Psi-\gamma_{th}\vartheta_1\right]}\right)\exp\left(-\left(\beta-\delta\right)x\right)dx, \tag{57}$$

$$Q_{33}\triangleq\sum_{q=1}^{N-1}(-1)^{q+1}\widetilde{\sum}\sum_{k=0}^{m_s-1}\frac{\alpha\zeta(k)\lambda_{\mathrm{RD}_n}}{\widetilde{\lambda}^{\mathrm{sum}}}\int_{\frac{\gamma_{th}\vartheta_1}{\Psi}}^{\infty}x^k\exp\left(-\frac{\left(\lambda_{\mathrm{RD}_n}+\lambda_{n,q}^{\mathrm{sum}}\right)\gamma_{th}\left[x\Psi\vartheta_3+\Xi\right]}{\Phi\left[x\Psi-\gamma_{th}\vartheta_1\right]}\right)\times\exp\left(-\left(\beta-\delta\right)x\right)dx. \tag{58}$$

From (56), the closed-form equation of $Q_{31}$ can be obtained as in (32). Based on (56) and by denoting $y=x\Psi-\gamma_{th}\vartheta_1$, $Q_{32}$ can be reformulated as

$$Q_{32}=\sum_{q=1}^{N-1}(-1)^{q+1}\widetilde{\sum}\sum_{k=0}^{m_s-1}\frac{\alpha\zeta(k)}{\Psi^{k+1}}\times\exp\left(-\frac{\left(\beta-\delta\right)\gamma_{th}\vartheta_1}{\Psi}-\frac{\lambda_{\mathrm{RD}_n}\gamma_{th}\vartheta_3}{\Phi}\right)\times\int_0^{\infty}\left[y+\gamma_{th}\vartheta_1\right]^k\exp\left(-\frac{\lambda_{\mathrm{RD}_n}\gamma_{th}\left[\gamma_{th}\vartheta_1\vartheta_3+\Xi\right]}{\Phi y}\right)\times\exp\left(-\frac{\left(\beta-\delta\right)y}{\Psi}\right)dy. \tag{59}$$

Owing to the Binomial Theorem $(x+y)^k=\sum_{p=0}^{k}\binom{k}{p}x^{k-p}y^p$, (59) can be rewritten by

$$Q_{32}=\sum_{q=1}^{N-1}(-1)^{q+1}\widetilde{\sum}\sum_{k=0}^{m_s-1}\sum_{p=0}^{k}\binom{k}{p}\frac{\alpha\zeta(k)[\gamma_{th}\vartheta_1]^{k-p}}{\Psi^{k+1}}\times\exp\left(-\frac{\left(\beta-\delta\right)\gamma_{th}\vartheta_1}{\Psi}-\frac{\lambda_{\mathrm{RD}_n}\gamma_{th}\vartheta_3}{\Phi}\right)\times\int_0^{\infty}y^p\exp\left(-\frac{\lambda_{\mathrm{RD}_n}\gamma_{th}\left[\gamma_{th}\vartheta_1\vartheta_3+\Xi\right]}{\Phi y}\right)\times\exp\left(-\frac{\left(\beta-\delta\right)y}{\Psi}\right)dy, \tag{60}$$

With the help of [44, eq.3.471.9], we can claim:

$$Q_{32}=2\sum_{q=1}^{N-1}(-1)^{q+1}\widetilde{\sum}\sum_{k=0}^{m_s-1}\sum_{p=0}^{k}\binom{k}{p}\frac{\alpha\zeta(k)[\gamma_{th}\vartheta_1]^{k-p}}{\Psi^{k+1}}\times\exp\left(-\frac{\left(\beta-\delta\right)\gamma_{th}\vartheta_1}{\Psi}-\frac{\lambda_{\mathrm{RD}_n}\gamma_{th}\vartheta_3}{\Phi}\right)\times\left\{\frac{\lambda_{\mathrm{RD}_n}\gamma_{th}\Psi\left[\gamma_{th}\vartheta_1\vartheta_3+\Xi\right]}{\Phi\left(\beta-\delta\right)}\right\}^{\frac{p+1}{2}}\times K_{p+1}\left(2\sqrt{\frac{\lambda_{\mathrm{RD}_n}\gamma_{th}\left(\beta-\delta\right)\left[\gamma_{th}\vartheta_1\vartheta_3+\Xi\right]}{\Phi\Psi}}\right), \tag{61}$$

where $K_p\left(\cdot\right)$ is the modified Bessel function of the second kind and $p^{th}$ order. By using the same approach as (61), the exact equation of $Q_{33}$ can be obtained as in (34). Based on (32), (61) and (34), $Q_3$ can be expressed as

$$Q_3=\sum_{q=1}^{N-1}(-1)^{q+1}\widetilde{\sum}\sum_{k=0}^{m_s-1}\sum_{p=0}^{k}\frac{\lambda_{n,q}^{\mathrm{sum}}}{\widetilde{\lambda}^{\mathrm{sum}}}\times\frac{\alpha\zeta(k)k!}{p!(\beta-\delta)^{(k+1-p)}}\times\left[\frac{\gamma_{th}\vartheta_1}{\Psi}\right]^p\exp\left(-\frac{\left(\beta-\delta\right)\gamma_{th}\vartheta_1}{\Psi}\right)-2\sum_{q=1}^{N-1}(-1)^{q+1}\widetilde{\sum}\sum_{k=0}^{m_s-1}\sum_{p=0}^{k}\binom{k}{p}\frac{\alpha\zeta(k)[\gamma_{th}\vartheta_1]^{k-p}}{\Psi^{k+1}}\times\left\{\frac{\gamma_{th}\Psi\left[\gamma_{th}\vartheta_1\vartheta_3+\Xi\right]}{\Phi\left(\beta-\delta\right)}\right\}^{\frac{p+1}{2}}\times\exp\left(-\frac{\left(\beta-\delta\right)\gamma_{th}\vartheta_1}{\Psi}\right)\times\left\{\begin{array}{l}\left(\lambda_{\mathrm{RD}_n}\right)^{\frac{p+1}{2}}\exp\left(-\frac{\lambda_{\mathrm{RD}_n}\gamma_{th}\vartheta_3}{\Phi}\right)\\\times K_{p+1}\left(2\sqrt{\frac{\lambda_{\mathrm{RD}_n}\gamma_{th}(\beta-\delta)[\gamma_{th}\vartheta_1\vartheta_3+\Xi]}{\Phi\Psi}}\right)\\-\lambda_{\mathrm{RD}_n}\left(\widetilde{\lambda}^{\mathrm{sum}}\right)^{\frac{p-1}{2}}\exp\left(-\frac{\widetilde{\lambda}^{\mathrm{sum}}\gamma_{th}\vartheta_3}{\Phi}\right)\\\times K_{p+1}\left(2\sqrt{\frac{\widetilde{\lambda}^{\mathrm{sum}}\gamma_{th}(\beta-\delta)[\gamma_{th}\vartheta_1\vartheta_3+\Xi]}{\Phi\Psi}}\right)\end{array}\right\}. \tag{62}$$

## Appendix B: Proof of Theorem 2

From (41), P can be rewritten as

$$\mathrm{P}=\underbrace{\int_0^{\infty}\Pr\left(\begin{array}{l}\gamma_{\mathrm{RE}_m}^{\mathrm{N-COL}}>Z_m,\\\frac{\Psi\Phi\gamma_{\mathrm{SR}}\gamma_{\mathrm{RE}_m}^{\mathrm{N-COL}}}{\gamma_{\mathrm{RE}_m}^{\mathrm{N-COL}}\Phi\vartheta_1+\gamma_{\mathrm{SR}}\Psi\vartheta_5+x\Theta\vartheta_1+\Lambda}<\gamma_{th}\end{array}\right)}_{\tilde{\mathrm{P}}}\times f_{\gamma_{\mathrm{JE}_m}}(x)dx, \tag{63}$$

where $\vartheta_5 \triangleq \left(\mu^2_{\mathrm{RE}_m}\Phi + \Theta\mu^2_{\mathrm{JE}_m} + x\Theta + 1\right)$. Next, $\tilde{\mathrm{P}}$ is calculated as

$$\begin{aligned}\tilde{\mathrm{P}} &= \Pr\left(\begin{array}{l}\gamma^{\mathrm{N-COL}}_{\mathrm{RE}_m} > Z_m, \\ \frac{\Psi\Phi\gamma_{\mathrm{SR}}\gamma^{\mathrm{N-COL}}_{\mathrm{RE}_m}}{\gamma^{\mathrm{N-COL}}_{\mathrm{RE}_m}\Phi\vartheta_1+\gamma_{\mathrm{SR}}\Psi\vartheta_5+x\Theta\vartheta_1+\Lambda} < \gamma_{th}\end{array}\right) \\ &= \Pr\left(\begin{array}{l}\gamma^{\mathrm{N-COL}}_{\mathrm{RE}_m} > Z_m, \\ \gamma^{\mathrm{N-COL}}_{\mathrm{RE}_m}\Phi\left[\Psi\gamma_{\mathrm{SR}} - \gamma_{th}\vartheta_1\right] \\ < \gamma_{th}\left[\gamma_{\mathrm{SR}}\Psi\vartheta_5 + x\Theta\vartheta_1 + \Lambda\right]\end{array}\right) \\ &= \underbrace{\Pr\left(\gamma^{\mathrm{N-COL}}_{\mathrm{RE}_m} > Z_m\right)\Pr\left[\Psi\gamma_{\mathrm{SR}} - \gamma_{th}\vartheta_1 \le 0\right]}_{\tilde{\mathrm{P}}_1} + \Upsilon, \quad (64)\end{aligned}$$

where the following definition holds

$$\Upsilon = \int_{\frac{\gamma_{th}\vartheta_1}{\Psi}}^{\infty} \underbrace{\Pr\left(Z_m < \gamma^{\mathrm{N-COL}}_{\mathrm{RE}_m} < \frac{\gamma_{th}\left[y\Psi\vartheta_5 + x\Theta\vartheta_1 + \Lambda\right]}{\Phi\left[y\Psi - \gamma_{th}\vartheta_1\right]}\right)}_{\tilde{\mathrm{P}}_2} \times f_{\gamma_{\mathrm{SR}}}(y)dy. \quad (65)$$

Based on (29), (30) and (64), $\tilde{\mathrm{P}}_1$ can be given by

$$\tilde{\mathrm{P}}_1 = \sum_{a=1}^{M-1}(-1)^{a+1}\widetilde{\sum^{M}}\frac{\lambda^{\mathrm{sum}}_{m,a}}{\widehat{\lambda}} \times \left\{\begin{array}{l}1 - \alpha\sum\limits_{k=0}^{m_s-1}\sum\limits_{p=0}^{k}\frac{\zeta(k)k!}{p!}(\beta-\delta)^{-(k+1-p)} \\ \times\left[\frac{\gamma_{th}\vartheta_1}{\Psi}\right]^p\exp\left(-\frac{\gamma_{th}\vartheta_1(\beta-\delta)}{\Psi}\right)\end{array}\right\}, \quad (66)$$

where $\widehat{\lambda} \triangleq \lambda^{\mathrm{sum}}_{m,a} + \lambda_{\mathrm{RE}_m}$. Similar proof as (54), $\tilde{\mathrm{P}}_2$ in (65) can be calculated by

$$\tilde{\mathrm{P}}_2 = \sum_{a=1}^{M-1}(-1)^{a+1}\widetilde{\sum^{M}}\left\{\begin{array}{l}\frac{\lambda^{\mathrm{sum}}_{m,a}}{\widehat{\lambda}} \\ -\exp\left(-\frac{\lambda_{\mathrm{RE}_m}\gamma_{th}\left[y\Psi\vartheta_5+x\Theta\vartheta_1+\Lambda\right]}{\Phi\left[y\Psi-\gamma_{th}\vartheta_1\right]}\right) \\ +\frac{\lambda_{\mathrm{RE}_m}}{\widehat{\lambda}}\exp\left(-\frac{\widehat{\lambda}\gamma_{th}\left[y\Psi\vartheta_5+x\Theta\vartheta_1+\Lambda\right]}{\Phi\left[y\Psi-\gamma_{th}\vartheta_1\right]}\right)\end{array}\right\}. \quad (67)$$

By substituting (67) into (65) and using the same approach for (56), $\Upsilon$ can be given as

$$\begin{aligned}\Upsilon &= \sum_{a=1}^{M-1}(-1)^{a+1}\widetilde{\sum^{M}}\sum_{k=0}^{m_s-1}\sum_{p=0}^{k}\frac{\lambda^{\mathrm{sum}}_{m,a}}{\widehat{\lambda}} \times \frac{\alpha\zeta(k)k!}{p!}(\beta-\delta)^{-(k+1-p)} \times \left[\frac{\gamma_{th}\vartheta_1}{\Psi}\right]^p \\ &\exp\left(-\frac{(\beta-\delta)\gamma_{th}\vartheta_1}{\Psi}\right) - 2\sum_{a=1}^{M-1}(-1)^{a+1} \\ &\widetilde{\sum^{M}}\sum_{k=0}^{m_s-1}\sum_{p=0}^{k}\binom{k}{p}\frac{\alpha\zeta(k)\left[\gamma_{th}\vartheta_1\right]^{k-p}}{\Psi^{k-p/2+1/2}\left[\Phi\left(\beta-\delta\right)\right]^{\frac{p+1}{2}}} \\ &\times\exp\left(-\frac{(\beta-\delta)\gamma_{th}\vartheta_1}{\Psi}\right) \\ &\times\left\{\begin{array}{l}\left[h_1(x)\right]^{\frac{p+1}{2}}\exp\left(-\frac{g_1(x)}{\Phi}\right) \\ \times K_{p+1}\left(2\sqrt{\frac{h_1(x)(\beta-\delta)}{\Phi\Psi}}\right) \\ -\frac{\lambda_{\mathrm{RE}_m}\left[h_2(x)\right]^{\frac{p+1}{2}}}{\widehat{\lambda}^{\mathrm{sum}}}\exp\left(-\frac{g_2(x)}{\Phi}\right) \\ \times K_{p+1}\left(2\sqrt{\frac{h_2(x)(\beta-\delta)}{\Phi\Psi}}\right)\end{array}\right\}, \quad (68)\end{aligned}$$

where

$$g_1(x) \triangleq \lambda_{\mathrm{RE}_m}\gamma_{th}\vartheta_5, \quad (69)$$

$$h_1(x) \triangleq \lambda_{\mathrm{RE}_m}\gamma_{th}\left[\gamma_{th}\vartheta_1\vartheta_5 + x\Theta\vartheta_1 + \Lambda\right], \quad (70)$$

$$g_2(x) \triangleq \widehat{\lambda}\gamma_{th}\vartheta_5, \quad (71)$$

$$h_2(x) \triangleq \widehat{\lambda}\gamma_{th}\left[\gamma_{th}\vartheta_1\vartheta_5 + x\Theta\vartheta_1 + \Lambda\right]. \quad (72)$$

By substituting (66) and (67) into (64), it yields

$$\begin{aligned}\tilde{\mathrm{P}} &= \sum_{a=1}^{M-1}(-1)^{a+1}\widetilde{\sum^{M}}\frac{\lambda^{\mathrm{sum}}_{m,a}}{\widehat{\lambda}} - 2\sum_{a=1}^{M-1}(-1)^{a+1} \\ &\times\widetilde{\sum^{M}}\sum_{k=0}^{m_s-1}\sum_{p=0}^{k}\binom{k}{p}\frac{\alpha\zeta(k)\left[\gamma_{th}\vartheta_1\right]^{k-p}}{\Psi^{k-p/2+1/2}\left[\Phi\left(\beta-\delta\right)\right]^{\frac{p+1}{2}}} \\ &\times\exp\left(-\frac{(\beta-\delta)\gamma_{th}\vartheta_1}{\Psi}\right) \\ &\times\left\{\begin{array}{l}\left[h_1(x)\right]^{\frac{p+1}{2}}\exp\left(-\frac{g_1(x)}{\Phi}\right) \\ \times K_{p+1}\left(2\sqrt{\frac{h_1(x)(\beta-\delta)}{\Phi\Psi}}\right) \\ -\frac{\lambda_{\mathrm{RE}_m}\left[h_2(x)\right]^{\frac{p+1}{2}}}{\widehat{\lambda}^{\mathrm{sum}}}\exp\left(-\frac{g_2(x)}{\Phi}\right) \\ \times K_{p+1}\left(2\sqrt{\frac{h_2(x)(\beta-\delta)}{\Phi\Psi}}\right)\end{array}\right\}. \quad (73)\end{aligned}$$

Finally, by substituting (73) into (63), the closed-form expression of $\mathrm{IP}^{\mathrm{AF}}$ can be expressed as in (46).

## Appendix C: Proof of Theorem 3

Based on (30), from (47) the $\mathrm{OP}_1$ can be calculated as

$$\begin{aligned}\mathrm{OP}_1 &= 1 - \Pr\left(\frac{\Psi\gamma_{\mathrm{SR}}}{\vartheta_1} < \gamma_{th}\right) = 1 - F_{\gamma_{\mathrm{SR}}}\left(\frac{\gamma_{th}\left[\vartheta_1\right]}{\Psi}\right) \\ &= \alpha\sum_{k=0}^{m_s-1}\sum_{p=0}^{k}\frac{\zeta(k)k!}{p!}(\beta-\delta)^{-(k+1-p)} \times \left[\frac{\gamma_{th}\left(\vartheta_1\right)}{\Psi}\right]^p \\ &\times\exp\left(-\frac{\gamma_{th}\vartheta_1\left(\beta-\delta\right)}{\Psi}\right). \quad (74)\end{aligned}$$

Next, the $\mathrm{OP}_2$ in (47) can be calculated as:

$$\begin{aligned}\mathrm{OP}_2 &= 1 - \sum_{n=1}^{N}\Pr\left(Z_n < \gamma_{\mathrm{RD}_n} < \frac{\gamma_{th}\vartheta_4}{\Phi}\right) \\ &= 1 - \sum_{n=1}^{N}\int_0^{\frac{\gamma_{th}\left(\Phi\mu^2_{\mathrm{RD}_n}+1\right)}{\Phi}} f_{Z_n}(z)\left[\exp\left(\begin{array}{l}-\lambda_{\mathrm{RD}_n}z \\ -\frac{\lambda_{\mathrm{RD}_n}\gamma_{th}\vartheta_4}{\Phi}\end{array}\right)\right]dz. \quad (75)\end{aligned}$$

By using the same approach as (55), (75) can be redefined as $\mathrm{OP}_2$

$$= 1 - \sum_{n=1}^{N}\sum_{q=1}^{N-1}(-1)^{q+1}\widetilde{\sum}\left\{\begin{array}{l}\frac{\lambda_{n,q}^{\mathrm{sum}}}{\widetilde{\lambda}^{\mathrm{sum}}} \\ -\exp\left(-\frac{\lambda_{\mathrm{RD}_n}\gamma_{th}\vartheta_4}{\Phi}\right) \\ +\frac{\lambda_{\mathrm{RD}_n}}{\widetilde{\lambda}^{\mathrm{sum}}}\exp\left(-\frac{\widetilde{\lambda}^{\mathrm{sum}}\gamma_{th}\vartheta_4}{\Phi}\right)\end{array}\right\}. \tag{76}$$

By substituting (76) and (74) into (47), the $\mathrm{OP}^{\mathrm{DF}}$ can be obtained as in (48). Thus, the proof is finished.

## Appendix D: Proof of Theorem 4

Based on (49), we can be written by

$$\mathrm{W} = \int_0^{\infty} \underbrace{\Pr\left(Z_m < \gamma_{\mathrm{RE}_m}^{\mathrm{N-COL}} < \frac{\gamma_{th}\vartheta_5}{\Phi}\right)}_{\tilde{\mathrm{W}}} f_{\gamma_{\mathrm{JE}_m}}(x)dx. \tag{77}$$

We observe that $\tilde{\mathrm{W}}$ in (77) can be computed as

$$\begin{aligned}\tilde{\mathrm{W}} &= \int_0^{\Xi_1}\int_z^{\Xi_1} f_{\gamma_{\mathrm{RE}_m}^{\mathrm{N-COL}}}(y) f_{Z_m}(z)dydz \\ &= \int_0^{\Xi_1} f_{Z_m}(z)\left[\exp\left(-\lambda_{\mathrm{RE}_m}z - \frac{\lambda_{\mathrm{RE}_m}\gamma_{th}\vartheta_5}{\Phi}\right)\right]dz \\ &= \sum_{a=1}^{M-1}(-1)^{a+1}\widetilde{\sum}^{M}\left\{\begin{array}{l}\frac{\lambda_{m,a}^{\mathrm{sum}}}{\widehat{\lambda}} \\ -\exp\left(-\frac{\lambda_{\mathrm{RE}_m}\gamma_{th}\vartheta_5}{\Phi}\right) \\ +\frac{\lambda_{\mathrm{RE}_m}}{\widehat{\lambda}}\exp\left(-\frac{\widehat{\lambda}\gamma_{th}\vartheta_5}{\Phi}\right)\end{array}\right\},\end{aligned} \tag{78}$$

where $\Xi_1 \triangleq \frac{\gamma_{th}\vartheta_5}{\Phi}$. By substituting (78) into (77), it yields

$$\begin{aligned}\mathrm{W} &= \sum_{a=1}^{M-1}(-1)^{a+1}\widetilde{\sum}^{M}\frac{\lambda_{m,a}^{\mathrm{sum}}}{\widehat{\lambda}} \\ &\quad - \sum_{a=1}^{M-1}(-1)^{a+1}\widetilde{\sum}^{M}\lambda_{\mathrm{JE}_m} \\ &\quad \times \exp\left(-\frac{\lambda_{\mathrm{RE}_m}\gamma_{th}\left(\Theta\mu_{\mathrm{JE}_m}^2 + \Phi\mu_{\mathrm{RE}_m}^2 + 1\right)}{\Phi}\right) \\ &\quad \times \int_0^{\infty}\exp\left[-x\left(\frac{\lambda_{\mathrm{RE}_m}\gamma_{th}\Theta}{\Phi} + \lambda_{\mathrm{JE}_m}\right)\right]dx \\ &\quad + \sum_{a=1}^{M-1}(-1)^{a+1}\widetilde{\sum}^{M}\frac{\lambda_{m,a}^{\mathrm{sum}}\lambda_{\mathrm{JE}_m}}{\widehat{\lambda}} \\ &\quad \exp\left(-\frac{\widehat{\lambda}\gamma_{th}\left(\Theta\mu_{\mathrm{JE}_m}^2 + \Phi\mu_{\mathrm{RE}_m}^2 + 1\right)}{\Phi}\right) \\ &\quad \times \int_0^{\infty}\exp\left[-x\left(\frac{\widehat{\lambda}\gamma_{th}\Theta}{\Phi} + \lambda_{\mathrm{JE}_m}\right)\right]dx,\end{aligned} \tag{79}$$

$$\begin{aligned}&= \sum_{a=1}^{M-1}(-1)^{a+1}\times \\ &\widetilde{\sum}^{M}\left\{\begin{array}{l}\frac{\lambda_{m,a}^{\mathrm{sum}}}{\widehat{\lambda}} - \frac{\lambda_{\mathrm{JE}_m}\Phi}{\lambda_{\mathrm{RE}_m}\gamma_{th}\Theta + \lambda_{\mathrm{JE}_m}\Phi} \\ \times\exp\left(-\frac{\lambda_{\mathrm{RE}_m}\gamma_{th}\left(\Theta\mu_{\mathrm{JE}_m}^2 + \Phi\mu_{\mathrm{RE}_m}^2 + 1\right)}{\Phi}\right) \\ +\frac{\lambda_{m,a}^{\mathrm{sum}}\lambda_{\mathrm{JE}_m}\Phi}{\widehat{\lambda}\left[\widehat{\lambda}\gamma_{th}\Theta + \Phi\lambda_{\mathrm{JE}_m}\right]} \\ \times\exp\left(-\frac{\widehat{\lambda}\gamma_{th}\left(\Theta\mu_{\mathrm{JE}_m}^2 + \Phi\mu_{\mathrm{RE}_m}^2 + 1\right)}{\Phi}\right)\end{array}\right\}.\end{aligned}$$

Substituting (79) into (49), the $\mathrm{IP}^{\mathrm{DF}}$ can be obtained as (50).

## References


[1] P. X. Nguyen, D.-H. Tran, O. Onireti, P. T. Tin, S. Q. Nguyen, S. Chatzinotas, and H. V. Poor, "Backscatter-assisted data offloading in OFDMA-based wireless-powered mobile edge computing for IoT networks," *IEEE Internet Things J.*, vol. 8, no. 11, pp. 9233–9243, June 2021.

[2] T. N. Nguyen, D.-H. Tran, T. Van Chien, V.-D. Phan, M. Voznak, P. T. Tin, S. Chatzinotas, D. W. K. Ng, and H. V. Poor, "Security-reliability trade-off analysis for SWIPT-and AF-based IoT networks with friendly jammers," *IEEE Internet of Things Journal*, vol. 9, no. 21, pp. 21 662 – 21 675, November 2022.

[3] Ericsson, "Ericsson mobility report: November 2020," November 2020.

[4] X. Huang, J. A. Zhang, R. P. Liu, Y. J. Guo, and L. Hanzo, "Airplane-aided integrated networking for 6G wireless: Will it work?" *IEEE Veh. Technol. Mag.*, vol. 14, no. 3, pp. 84–91, July 2019.

[5] B. Mao, Y. Kawamoto, and N. Kato, "AI-based joint optimization of QoS and security for 6G energy harvesting internet of things," *IEEE Internet Things J.*, vol. 7, no. 8, pp. 7032–7042, August 2020.

[6] T. Van Chien, E. Lagunas, T. H. Ta, S. Chatzinotas, and B. Ottersten, "User scheduling and power allocation for precoded multi-beam high throughput satellite systems with individual quality of service constraints," *IEEE Transactions on Vehicular Technology*, vol. 72, no. 1, pp. 907–923, January 2023.

[7] B. Di, L. Song, Y. Li, and H. V. Poor, "Ultra-dense LEO: Integration of satellite access networks into 5G and beyond," *IEEE Wireless Commun.*, vol. 26, no. 2, pp. 62–69, April 2019.

[8] B. C. Nguyen, T. M. Hoang, P. T. Tran, and T. N. Nguyen, "Outage probability of NOMA system with wireless power transfer at source and full-duplex relay," *AEU-international Journal of Electronics and Communications*, vol. 116, p. 152957, March 2020.

[9] P. T. Tin, T. N. Nguyen, D.-H. Tran, M. Voznak, V.-D. Phan, and S. Chatzinotas, "Performance enhancement for full-duplex relaying with time-switching-based SWIPT in wireless sensors networks," *Sensors*, vol. 21, no. 11, p. 3847, June 2021.

[10] T. N. Nguyen, M. Tran, T. Nguyen, and M. Voznak, "Adaptive relaying protocol for decode and forward full-duplex system over Rician fading channel: System performance analysis," *China Commun.*, vol. 16, no. 3, pp. 92–102, March 2019.

[11] T. N. Nguyen, P. T. Tran, and M. Voznak, "Wireless energy harvesting meets receiver diversity: A successful approach for two-way half-duplex relay networks over block rayleigh fading channel," *Comput. Netw.*, vol. 172, p. article no. 107176, May 2020.

[12] H. Dinh Tran, D. Trung Tran, and S. G. Choi, "Secrecy performance of a generalized partial relay selection protocol in underlay cognitive networks," *Int. J. Commun. Syst.*, vol. 31, no. 17, p. e3806, September 2018.

[13] J. Chamberlain and R. Medhurst, "Mutual interference between communication satellites and terrestrial line-of-sight radio-relay systems," vol. 111, no. 3, pp. 524–534, March 1964.

[14] J. Chamberlain, "Interference between an earth station of a communication-satellite system and the stations of terrestrial line-of-sight radio-relay systems," vol. 112, no. 2, pp. 231–241, February 1965.

[15] P. Johns, "Interference between terrestrial line-of-sight radio-relay systems and communication-satellite systems," *Electronics Letters*, vol. 2, no. 5, pp. 177–178, May 1966.

[16] J. Lee, "Symbiosis between a terrestrial-based integrated services digital network and a digital satellite network," *IEEE J. Sel. Areas Commun.*, vol. 1, no. 1, pp. 103–109, January 1983.

[17] C. Caini, G. E. Corazza, G. Falciasecca, M. Ruggieri, and F. Vatalaro, "A spectrum-and power-efficient EHF mobile satellite system to be integrated with terrestrial cellular systems," *IEEE J. sel. areas commun.*, vol. 10, no. 8, pp. 1315–1325, October 1992.

[18] V.-P. Bui, T. Van Chien, E. Lagunas, J. Grotz, S. Chatzinotas, and B. Ottersten, "Robust congestion control for demand-based optimization in precoded multi-beam high throughput satellite communications," *IEEE Transactions on Communications*, vol. 70, no. 10, pp. 6918–6937, 2022.

[19] M. R. Bhatnagar, "Making two-way satellite relaying feasible: A differential modulation based approach," *IEEE Trans. Commun.*, vol. 63, no. 8, pp. 2836–2847, August 2015.

[20] W. Zeng, J. Zhang, D. W. K. Ng, B. Ai, and Z. Zhong, "Two-way hybrid terrestrial-satellite relaying systems: Performance analysis and relay selection," *IEEE Trans. Veh. Technol.*, vol. 68, no. 7, pp. 7011–7023, July 2019.

[21] K. Guo, B. Zhang, Y. Huang, and D. Guo, "Performance analysis of two-way satellite terrestrial relay networks with hardware impairments," *IEEE Wireless Commun. Lett.*, vol. 6, no. 4, pp. 430–433, August 2017.

[22] H. Dong, C. Hua, L. Liu, and W. Xu, "Towards integrated terrestrial-satellite network via intelligent reflecting surface," in *Proc. ICC 2021*, June 2021, pp. 1–6.

[23] P. K. Sharma, D. Gupta, and D. I. Kim, "Outage performance of 3D mobile UAV caching for hybrid satellite-terrestrial networks," *IEEE Trans. Veh. Technol.*, vol. 70, no. 8, pp. 8280–8285, August 2021.

[24] D.-H. Tran, S. Chatzinotas, and B. Ottersten, "Satellite-and Cache-assisted UAV: A Joint Cache Placement, Resource Allocation, and Trajectory Optimization for 6G Aerial Networks," *IEEE Open Journal of Vehicular Technology*, vol. 3, pp. 40–54, January 2022.

[25] N. Hoang An, M. Tran, T. N. Nguyen, and D.-H. Ha, "Physical layer security in a hybrid TPSR two-way half-duplex relaying network over a rayleigh fading channel: Outage and intercept probability analysis," *Electronics*, vol. 9, no. 3, p. 428, March 2020.

[26] T. Dinh Hieu, T. T. Duy, and S. G. Choi, "Performance enhancement for harvest-to-transmit cognitive multi-hop networks with best path selection method under presence of eavesdropper," in *Proc. ICACT*, February 2018, pp. 323–328.

[27] D. H. Ha, T. N. Nguyen, M. H. Q. Tran, X. Li, P. T. Tran, and M. Voznak, "Security and reliability analysis of a two-way half-duplex wireless relaying network using partial relay selection and hybrid TPSR energy harvesting at relay nodes," *IEEE Access*, vol. 8, pp. 187 165–187 181, October 2020.

[28] D. H. Tran, T. T. Duy, and B. Kim, "Performance enhancement for multihop harvest-to-transmit WSNs with path-selection methods in presence of eavesdroppers and hardware noises," *IEEE Sens. J.*, vol. 18, no. 12, pp. 5173–5186, June 2018.

[29] V. Bankey and P. K. Upadhyay, "Physical layer security of multiuser multirelay hybrid satellite-terrestrial relay networks," *IEEE Trans. Veh. Technol.*, vol. 68, no. 3, pp. 2488–2501, March 2019.

[30] A. Kalantari, G. Zheng, Z. Gao, Z. Han, and B. Ottersten, "Secrecy analysis on network coding in bidirectional multibeam satellite communications," *IEEE Trans. Inf. Forensics Secur.*, vol. 10, no. 9, pp. 1862–1874, September 2015.

[31] P. K. Sharma and D. I. Kim, "Secure 3D mobile UAV relaying for hybrid satellite-terrestrial networks," *IEEE Trans. Wireless Commun.*, vol. 19, no. 4, pp. 2770–2784, April 2020.

[32] S. Xu, J. Liu, Y. Cao, J. Li, and Y. Zhang, "Intelligent reflecting surface enabled secure cooperative transmission for satellite-terrestrial integrated network," *IEEE Trans. Veh. Technol.*, vol. 70, no. 2, pp. 2007–2011, February 2021.

[33] K.-B. Yu, "Adaptive beamforming for satellite communication with selective earth coverage and jammer nulling capability," *IEEE Trans. Signal Process.*, vol. 44, no. 12, pp. 3162–3166, December 1996.

[34] M. Bouabdellah and F. El Bouanani, "A PHY layer security of a jamming-based underlay cognitive satellite-terrestrial network," *IEEE Trans. Cogn. Commun. Netw*, vol. 7, no. 4, pp. 1266–1279, December 2021.

[35] V. Bankey and P. K. Upadhyay, "Improving secrecy performance of land mobile satellite systems via a UAV friendly jammer," in *Proc. CCNC*, January 2020, pp. 1–4.

[36] T. N. Nguyen, D.-H. Tran, T. Van Chien, V.-D. Phan, M. Voznak, and S. Chatzinotas, "Security and reliability analysis of satellite-terrestrial multirelay networks with imperfect CSI," *IEEE Systems Journal*, 2022.

[37] T. Van Chien, E. Lagunas, T. M. Hoang, S. Chatzinotas, B. Ottersten, and L. Hanzo, "Space-terrestrial cooperation over spatially correlated channels relying on imperfect channel estimates: Uplink performance analysis and optimization," *IEEE Transactions on Communications*, vol. 71, no. 2, pp. 773 – 791, 2023.

[38] X. Li, W. Feng, Y. Chen, C.-X. Wang, and N. Ge, "Maritime coverage enhancement using UAVs coordinated with hybrid satellite-terrestrial networks," *IEEE Trans. Commun.*, vol. 68, no. 4, pp. 2355–2369, April 2020.

[39] X. Gao, O. Edfors, F. Rusek, and F. Tufvesson, "Massive MIMO performance evaluation based on measured propagation data," *IEEE Transactions on Wireless Communications*, vol. 14, no. 7, pp. 3899–3911, July 2015.

[40] M. K. Samimi, S. Sun, and T. S. Rappaport, "MIMO channel modeling and capacity analysis for 5G millimeter-wave wireless systems," in *Proc. EuCAP*. IEEE, April 2016, pp. 1–5.

[41] K. An, M. Lin, T. Liang, J.-B. Wang, J. Wang, Y. Huang, and A. L. Swindlehurst, "Performance analysis of multi-antenna hybrid satellite-terrestrial relay networks in the presence of interference," *IEEE Trans. Commun.*, vol. 63, no. 11, pp. 4390–4404, November 2015.

[42] A. Abdi, W. C. Lau, M.-S. Alouini, and M. Kaveh, "A new simple model for land mobile satellite channels: First-and second-order statistics," *IEEE Transactions on Wireless Communications*, vol. 2, no. 3, pp. 519–528, May 2003.

[43] M. R. Bhatnagar and A. M.K., "Performance analysis of AF based hybrid satellite-terrestrial cooperative network over generalized fading channels," *IEEE Communications Letters*, vol. 17, no. 10, pp. 1912–1915, October 2013.

[44] A. Jeffrey and D. Zwillinger, *Table of integrals, series, and products - Seventh edition*. Elsevier, February 2007.

[45] P. K. Upadhyay and P. K. Sharma, "Max-max user-relay selection scheme in multiuser and multirelay hybrid satellite-terrestrial relay systems," *IEEE Commun. Lett.*, vol. 20, no. 2, pp. 268–271, February 2016.

[46] N. Cassiau, G. Noh, S. Jaeckel, L. Raschkowski, J.-M. Houssin, L. Combelles, M. Thary, J. Kim, J.-B. Doré, and M. Laugeois, "Satellite and terrestrial multi-connectivity for 5G: making spectrum sharing possible," in *Proc. WCNCW*. IEEE, April 2020, pp. 1–6.

[47] F. Boulos, S. Caizzone, and A. Winterstein, "A subarray-based antenna design for satellite communications ground terminals in Ka band," in *Proc. Ka and Broadband Communications Conference*, April 2021.

[48] A. T. Muriel-Barrado, J. Calatayud-Maeso, A. Rodríguez-Gallego, P. Sánchez-Olivares, J. M. Fernández-González, and M. Sierra-Pérez, "Evaluation of a planar reconfigurable phased array antenna driven by a multi-channel beamforming module at Ka band," *IEEE Access*, vol. 9, pp. 63 752–63 766, April 2021.

[49] X. Li, M. Huang, C. Zhang, D. Deng, K. M. Rabie, Y. Ding, and J. Du, "Security and reliability performance analysis of cooperative multi-relay systems with nonlinear energy harvesters and hardware impairments," *IEEE Access*, vol. 7, pp. 102 644–102 661, July 2019.

[50] T. N. Nguyen, D.-T. Do, P. T. Tran, and M. Voznak, "Time switching for wireless communications with full-duplex relaying in imperfect CSI condition," *KSII T. Internet Info.*, vol. 10, no. 9, pp. 4223–4239, September 2016.

[51] Q. Huang, M. Lin, K. An, J. Ouyang, and W.-P. Zhu, "Secrecy performance of hybrid satellite-terrestrial relay networks in the presence of multiple eavesdroppers," *IET Commun.*, vol. 12, pp. 26–34, January 2018.

[52] N. T. Do, V. N. Q. Bao, and B. An, "Outage performance analysis of relay selection schemes in wireless energy harvesting cooperative networks over non-identical Rayleigh fading channels," *Sensors*, vol. 16, no. 3, February 2016. [Online]. Available: https://www.mdpi.com/1424-8220/16/3/295

[53] Y. Huang, F. S. Al-Qahtani, T. Q. Duong, and J. Wang, "Secure transmission in MIMO wiretap channels using general-order transmit antenna selection with outdated CSI," *IEEE Trans. Commun.*, vol. 63, no. 8, pp. 2959–2971, August 2015.

[54] L. Fan, X. Lei, T. Q. Duong, M. Elkashlan, and G. K. Karagiannidis, "Secure multiuser multiple amplify-and-forward relay networks in presence of multiple eavesdroppers," in *Proc. 2014 IEEE Global Communications Conference*, December 2014, pp. 4120–4125.

[55] Y.-U. Jang and Y. H. Lee, "Performance analysis of user selection for multiuser two-way amplify-and-forward relay," *IEEE Commun. Lett.*, vol. 14, no. 11, pp. 1086–1088, November 2010.

[56] X. Li, M. Zhao, Y. Liu, L. Li, Z. Ding, and A. Nallanathan, "Secrecy analysis of ambient backscatter NOMA systems under I/Q imbalance," *IEEE Trans. Veh. Technol.*, vol. 69, no. 10, pp. 12 286–12 290, October 2020.

[57] Y. Zou, B. Champagne, W.-P. Zhu, and L. Hanzo, "Relay-selection improves the security-reliability trade-off in cognitive radio systems," *IEEE Trans. Commun.*, vol. 63, no. 1, pp. 215–228, January 2015.
[58] Y. Zou, "Intelligent interference exploitation for heterogeneous cellular networks against eavesdropping," *IEEE J. Sel. Areas Commun.*, vol. 36, no. 7, pp. 1453–1464, July 2018.
[59] T. N. Nguyen, L.-T. Tu, D.-H. Tran, V.-D. Phan, M. Voznak, S. Chatzinotas, and Z. Ding, "Outage performance of satellite terrestrial full-duplex relaying networks with co-channel interference," *IEEE Wireless Communications Letters*, vol. 11, no. 7, pp. 1478–1482, July 2022.
[60] T. Van Chien, L. T. Tu, S. Chatzinotas, and B. Ottersten, "Coverage probability and ergodic capacity of intelligent reflecting surface-enhanced communication systems," *IEEE Communications Letters*, vol. 25, no. 1, pp. 69–73, January 2020.

**Tan N. Nguyen** was born at Nha Trang City, Vietnam, in 1986. He received B.S. and M.S. degrees in electronics and telecommunications engineering from Ho Chi Minh University of Natural Sciences, a member of Vietnam National University at Ho Chi Minh City (Vietnam) in 2008 and 2012, respectively. He is currently pursuing his Ph.D. degree in electrical engineering at VSB Technical University of Ostrava, Czech Republic. He got his Ph.D. degree in computer science, communication technology and applied mathematics at VSB Technical University of Ostrava, Czech Republic, in 2019. In 2013, he joined the Faculty of Electrical and Electronics Engineering of Ton Duc Thang University, Vietnam and have been working as lecturer since then. His major interests are cooperative communications, cognitive radio, and physical layer security.

**Trinh Van Chien** (S'16-M'20) received the B.S. degree in Electronics and Telecommunications from Hanoi University of Science and Technology (HUST), Vietnam, in 2012. He then received the M.S. degree in Electrical and Computer Enginneering from Sungkyunkwan University (SKKU), Korea, in 2014 and the Ph.D. degree in Communication Systems from Linköping University (LiU), Sweden, in 2020. He was a research associate at University of Luxembourg. He is now with the School of Information and Communication Technology (SoICT), Hanoi University of Science and Technology (HUST), Vietnam. His interest lies in convex optimization problems and machine learning applications for wireless communications and image & video processing. He was an IEEE wireless communications letters exemplary reviewer for 2016, 2017 and 2021. He also received the award of scientific excellence in the first year of the 5Gwireless project funded by European Union Horizon's 2020.

**Dinh-Hieu TRAN** (S'20) was born and grew up in Gia Lai, Vietnam (1989). He received a B.E. degree in Electronics and Telecommunication Engineering Department from Ho Chi Minh City University of Technology, Vietnam, in 2012. He finished his M.Sc degree in Electronics and Computer Engineering from Hongik University, Korea, in 2017, and the Ph.D. degree in Telecommunications Engineering from the Interdiscipline Reliability and Trust (SnT) research center, the University of Luxembourg in December 2021, under the supervision of Prof. Symeon Chatzinotas and Prof. Björn Ottersten. His major interests include UAV, Satellite, IoT, Mobile Edge Computing, Caching, B5G for wireless communication networks. In 2016, he received the Hongik Rector Award for his excellence during his master's study at Hongik University. He was a co-recipient of the IS3C 2016 best paper award. In 2021, he was nominated for the Best Ph.D. Thesis Award at the University of Luxembourg.

**Van-Duc Phan** (duc.pv@vlu.edu.vn) was born in 1975 in Long An province, Vietnam. He received his M.S. degree in Department of Electric, Electrical and Telecommunication Engineering from Ho Chi Minh City University of Transport, Ho Chi Minh, Vietnam and Ph.D. degree in Department of Mechanical and Automation Engineering, Da-Yeh University, Taiwan in 2016. Currently, he is a research interests are in sliding mode control, non-linear systems or active manegtic bearing, flywheel store energy systems, power system optimization, optimization algorithms, and renewable energies, Energy harvesting (EH) enabled cooperative networks, Improving the optical properties, lighting performance of white LEDs, Energy efficiency LED driver integrated circuits, Novel radio access technologies, Physical security in communication network.

**MIROSLAV VOZNAK** (M'09-SM'16) received his PhD in telecommunications in 2002 from the Faculty of Electrical Engineering and Computer Science at VSB -Technical University of Ostrava, and achieved habilitation in 2009. He was appointed Full Professor in Electronics and Communications Technologies in 2017. His research interests generally focus on ICT, especially on quality of service and experience, network security, wireless networks, and big data analytics. He has authored and co-authored over one hundred articles indexed in SCI/SCIE journals. According to the Stanford University study released in 2020, he is one of the researchers who belong to Top 2 % of scientists in Networking & Telecommunications and Information & Communications Technologies. He served as a general chair of the 11th IFIP Wireless and Mobile Networking Conference in 2018 and the 24th IEEE/ACM International Symposium on Distributed Simulation and Real Time Applications in 2020. He participated in six projects funded by EU in programs managed directly by European Commission. Currently, he is a principal investigator in the research project QUANTUM5 funded by NATO, which focuses on the application of quantum cryptography in 5G campus networks.

**Symeon Chatzinotas** (S'06, M'09, SM'13, F'23) is Full Professor and Head of the SIGCOM Research Group at SnT, University of Luxembourg. He is coordinating the research activities on communications and networking across a group of 80 researchers, acting as a PI for more than 40 projects and main representative for 3GPP, ETSI, DVB. He is currently serving in the editorial board of the IEEE Transactions on Communications, IEEE Open Journal of Vehicular Technology and the International Journal of Satellite Communications and Networking. In the past, he has been a Visiting Professor at the University of Parma, Italy and was involved in numerous R&D projects for NCSR Demokritos, CERTH Hellas and CCSR, University of Surrey. He was the co-recipient of the 2014 IEEE Distinguished Contributions to Satellite Communications Award and Best Paper Awards at WCNC, 5GWF, EURASIP JWCN, CROWNCOM, ICSSC. He has (co-)authored more than 700 technical papers in refereed international journals, conferences and scientific books.

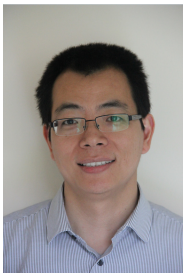

**Zhiguo Ding** (S'03-M'05-F'20) received his B.Eng from the Beijing University of Posts and Telecommunications in 2000, and the Ph.D degree from Imperial College London in 2005. He is currently a Professor in Communications at Khalifa University, and has also been affiliated with the University of Manchester and Princeton University. Dr Ding' research interests are 6G networks, multiple access, energy harvesting networks and statistical signal processing. He is serving as an Area Editor for the *IEEE Transactions on Wireless Communications*, and *IEEE Open Journal of the Communications Society*, an Editor for *IEEE Transactions on Vehicular Technology*, and was an Editor for *IEEE Wireless Communication Letters*, *IEEE Transactions on Communications*, *IEEE Communication Letters* from 2013 to 2016. He recently received the EU Marie Curie Fellowship 2012-2014, the Top IEEE TVT Editor 2017, IEEE Heinrich Hertz Award 2018, IEEE Jack Neubauer Memorial Award 2018, IEEE Best Signal Processing Letter Award 2018, Friedrich Wilhelm Bessel Research Award 2020, and IEEE SPCC Technical Recognition Award 2021. He is a Fellow of the IEEE, a Distinguished Lecturer of IEEE ComSoc, and a Web of Science Highly Cited Researcher in two categories 2022.

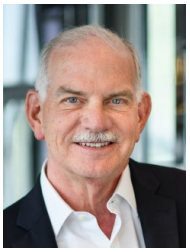

**H. Vincent Poor** (S'72, M'77, SM'82, F'87) received the Ph.D. degree in EECS from Princeton University in 1977. From 1977 until 1990, he was on the faculty of the University of Illinois at Urbana-Champaign. Since 1990 he has been on the faculty at Princeton, where he is currently the Michael Henry Strater University Professor. During 2006 to 2016, he served as the dean of Princeton's School of Engineering and Applied Science. He has also held visiting appointments at several other universities, including most recently at Berkeley and Cambridge. His research interests are in the areas of information theory, machine learning and network science, and their applications in wireless networks, energy systems and related fields. Among his publications in these areas is the forthcoming book Machine Learning and Wireless Communications. (Cambridge University Press). Dr. Poor is a member of the National Academy of Engineering and the National Academy of Sciences and is a foreign member of the Chinese Academy of Sciences, the Royal Society, and other national and international academies. He received the IEEE Alexander Graham Bell Medal in 2017.